REPORT METEOROLOGY AND CLIMATOLOGY No. 119, 2023

Quantification of population exposure to PM10, PM2.5 and NO_2 and estimated health impacts for 2019 and 2030

A study based on high resolution dispersion modelling

Helene Alpfjord Wylde[1], Christian Asker[1], Cecilia Bennet[1], Bertil Forsberg[2], David Segersson[1]

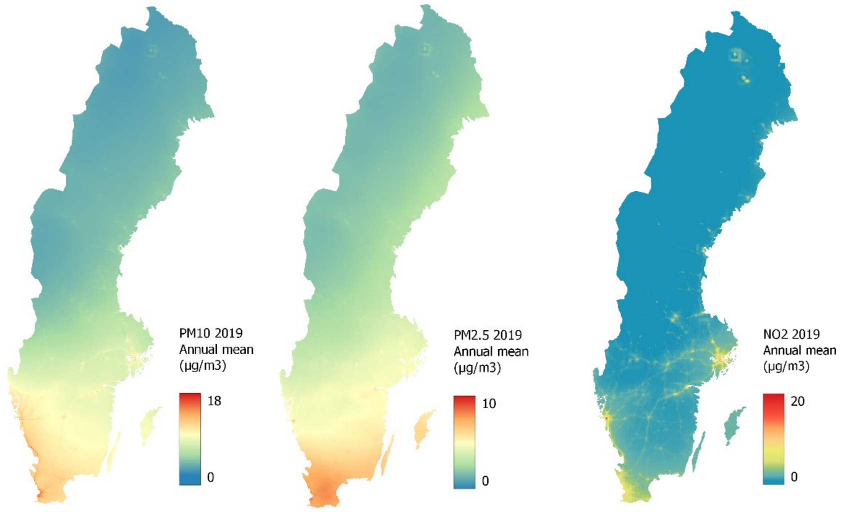

[1] SMHI

[2] Umeå University

Front:
Annual mean concentrations of PM10, PM2.5 and NO_2 over Sweden for 2019.

ISSN: 0347-2116

REPORT METEOROLOGY AND CLIMATOLOGY No. 119, 2023

Quantification of population exposure to PM10, PM2.5 and NO_2 and estimated health impacts for 2019 and 2030

A study based on high resolution dispersion modelling

Helene Alpfjord Wylde, Christian Asker, Cecilia Bennet, Bertil Forsberg, David Segersson

Reviewer: Maria Grundström
Department: Professional Services, SMHI
Client: Maria Ullerstam, Naturvårdsverket (Swedish EPA)

Summary

Concentrations of NO_2, PM10 and PM2.5 have been calculated for the whole of Sweden for the year 2019 as well as two scenarios for 2030 in this study. Calculations have been performed using a new methodology, allowing almost seam-less combination of dispersion modelling at regional and urban scale without double-counting emissions. The concentrations have been calculated at 250x250 m^2 resolution, producing a uniquely complete and detailed dataset at national scale. The methodology used can well reproduce the measured pollution levels at most urban background stations in the modelling domain. The spatial resolution of 250 m captures concentration gradients that are of importance for exposure calculations. An important strength of using dispersion modelling to calculate concentrations is the direct relation with emission inventories, allowing for source attribution and scenario evaluation that is consistent with emission inventories and projections.

The modelled concentrations are used together with gridded population data in order to calculate exposure. The annual average population weighted exposure is 5.08 µg/m^3 for NO_2, 9.95 µg/m^3 for PM10 and 5.21 µg/m^3 for PM2.5 in 2019. A large decrease, by approximately 2 µg/m^3**,** is seen for exposure to NO_2 in 2030 compared to 2019. The exposure to PM10 and PM2.5 is also decreasing in 2030, but not as drastically, by about 0.2 µg/m^3.

A general conclusion is that exposure is higher in the age span of 21-50 years. An explanation is that these age groups more often live in urban areas, where there are more emissions and higher concentrations of pollution.

Zero percent of the population is exposed to levels above the annual air quality standards for NO_2, PM10 and PM2.5 for 2019 and 2030. It is to be noted that the model results represent annual averaged urban background concentrations, not local hotspot concentrations.

The modelled exposures to PM2.5 and urban NO_2 have been used for a national health impact assessment. The health impact assessment is similar to an earlier study of premature deaths and incident cases of mainly chronic diseases. Our results differ to a varying degree from similar impact assessments. Most important among the complicated reasons for differences in the estimated health impacts are the assumed exposure-response functions for the specific exposures, the slope and if there is a lower threshold below which no association exists. We have in this study decided to follow the strong evidence from high quality epidemiological studies that the exposure-response relationship between long-term exposure to PM2.5 and total mortality in adults is supra-linear with a much steeper slope at the lower end, with stronger effects of near source exposure, and no evidence of a threshold level below which no effects are observed. When adding the yearly number of premature deaths attributed to the regional background PM2.5 levels and the deaths associated with PM2.5 exposure from local sources, the total number becomes 4 264 deaths related to the fine particle exposure situation in 2019. At the same time, the urban contribution of NO_2 is estimated to result in additional 428 premature deaths per year.

In 2030 the population exposure to PM2.5 from the regional background is expected to be about 2% lower and from urban sources 22% lower compared to 2019, which indicates how much the attributed number of preterm deaths would change if everything else stays the same.

Sammanfattning

Halter av NO_2, PM10 och PM2.5 har beräknats för hela Sverige för år 2019 och för två scenarier 2030 i den här studien. Beräkningar har gjorts med en ny metodik som möjliggör en nästan helt sömlös kombination av spridningsmodellering på regional och urban skala utan att dubbelräkna emissioner. Föroreningshalter har beräknats på 250x250 m^2 upplösning, vilket ger ett unikt komplett och detaljerat dataset på nationell skala. Metodiken kan väl reproducera uppmätta föroreningshalter vid de flesta urbana bakgrundsstationerna i modelldomänet. Den spatiala upplösningen på 250 m fångar koncentrationsgradienter av vikt för exponeringsberäkningar. En styrka med att använda spridningsmodeller för att beräkna föroreningshalter är den direkta kopplingen till emissionsinventeringar och projektioner.

Modellerade föroreningshalter kombineras med griddad befolkningsdata för att beräkna exponering. Den befolkningsviktade årsmedelexponeringen är 5,08 $\mu g/m^3$ för NO_2, 9,95 $\mu g/m^3$ för PM10 och 5,21 $\mu g/m^3$ för PM2.5 år 2019. En stor minskning, med cirka 2 $\mu g/m^3$ till 2030, beräknas för exponering av NO_2. Exponeringen för PM10 och PM2.5 minskar också till 2030, men inte lika drastiskt, med ungefär 0,2 $\mu g/m^3$.

En generell slutsats är att exponeringen är högre i åldersspannet 21-50 år. En förklaring är dessa åldersgrupper oftare bor i urbana områden, med mer utsläpp och högre föroreningshalter.

Noll procent av befolkningen exponeras för halter över den årliga miljökvalitetsnormen för NO_2, PM10 och PM2.5, varken år 2019 eller 2030. Det ska dock noteras att modellresultaten representerar årsmedelvärden av urbana bakgrundskoncentrationer, inte lokala hotspots.

De modellbaserade beräkningarna av exponeringen för PM2.5 och lokalt genererad NO_2 har använts i en nationell hälsokonsekvensberäkning. Hälsokonsekvensberäkningen liknar en nyligen publicerad beräkning avseende 2019, av förtida dödsfall och uppkomst av främst kroniska sjukdomar. Våra resultat avviker i olika riktning från resultaten i liknande beräkningar. En avgörande och komplicerad anledning till skillnader i de beräknade hälsokonsekvenserna är vilka exponerings-responssamband för specifika föroreningar som man baserar sina beräkningar på, riskkurvans form och om det finns någon säker nivå under vilken sambandet upphör. I denna studie har vi valt att luta oss mot den vetenskapliga evidens som ges av högkvalitativa epidemiologiska studier för att sambanden mellan partikelhalt och dödlighet är supra-linjära med den brantaste riskökningen vid de lägsta halterna, att effekterna är starkare nära källan samt att det inte finns stöd för någon tröskelnivå under vilken halten saknar betydelse. När vi räknar ihop antal förtida dödsfall per år som den regionala bakgrundshalten av PM2.5 beräknas orsaka med de dödsfall som beräknas uppkomma till följd av partikelutsläpp på hemorten så blir summan 4 264 förtida dödsfall relaterade till föroreningssituationen 2019. För samma exponeringssituation uppskattar vi att de lokalt genererade bidraget till NO_2-halten leder till ytterligare 428 förtida dödsfall per år.

2030 beräknas befolkningsexponeringen för PM2.5 från den regionala bakgrunden ha minskat med omkring 2 % och från urbana källor med 22 % jämfört med 2019, vilket indikerar hur mycket antalet förtida dödsfall skulle reduceras om allt övrigt är oförändrat.

Table of contents

1 Background

Although air quality in Sweden has improved over the past decades limit values for air quality are still being exceeded in some urban areas. Negative effects on human health due to exposure of increased levels of air pollution still results in high socio-economic costs on a national scale. Quantification of exposure to air pollution in both 2019 and 2030 on a national scale is valuable to evaluate progress made and the need of further actions to improve air quality.

In 2021 the World Health Organization (WHO) presented new updated air quality guidelines including recommendations for air quality levels to protect public health from adverse effects from air pollution. The new guidelines were a result of a review of the latest scientific knowledge which provided clear evidence that air pollution affects health at lower concentrations than previously understood. The new guidelines were used as a base for the proposal for a revised air quality directive with stricter air quality limits which was presented by the EU Commission in October 2022. The negotiation of the proposal is expected to start during spring 2023.

Air policies aim to reduce exposure to air pollution by setting limit and target values for air quality together with reducing emissions. All EU member states have national reduction commitments until 2030 for air pollutants through the so-called NEC directive. Member states shall produce and implement national air pollution control programmes which have to be updated at a minimum every fourth year as a tool to reach their reduction commitments.

Sweden reported their first national programme to the EU in April 2019. According to the national emission inventory and scenarios for air pollutants Sweden needs to implement policies and measures to further reduce emissions of NO_x and ammonia to reach their national reduction target for 2030. The Swedish National Air Pollution Control Programme contains two action areas for reduction of emissions of NO_x and one action area for reduction of emissions of ammonia. One of the action areas regarding NO_x includes emissions from industry and district heating and the other one emissions from national transport. An updated version should be established and reported to the EU during 2023.

National quantifications of population exposure based on air quality modelling can be useful in several areas. SMHI has developed a new dispersion modelling approach, based on the regional model MATCH and the CLAIR platform. This modelling approach allows for national air quality assessments with high quality and high resolution. These assessments provide improved data for health studies and cost analyses. Dispersion results can be further used for assessing the potential of actions in the Swedish National Air Pollution Control Programme, as well as supporting action plans and evaluating the progress towards achievement of the Swedish environmental objectives.

2 Aim

The aim of the project was to do a national quantification of population exposure to NO_2, $PM_{2.5}$ and PM_{10} for the year of 2019 and the scenario year of 2030 in urban background. The year of 2019 was used as a baseline to avoid effects of the Covid-19 pandemic on the air quality. The exposure results were delivered to Umeå University, responsible for the health impact calculations.

The results from this study will be an important input when assessing the effects of expected reduction of NO_x emissions between today and 2030 with present policies and measures and measures according to the Swedish National Air Pollution Control Programme. It can also be used to evaluate possible effects of stricter limit values for air quality and the progress towards achievement of the Swedish environmental objectives for clean air.

3 Methodology

Calculations in this study follow the so called impact pathway (Segersson, 2021), presented in Figure 1. All steps along the pathway are described below, from emission preparation and dispersion modelling on regional and urban scale, to population exposure and health impact assessment.

For year 2019, concentrations calculated using dispersion modelling are adjusted using observations, both on a regional and urban scale.

Calculations are made for the baseline year 2019, as well as for two different scenarios for 2030. The scenarios are also adjusted for observations from 2019, in order to make the different datasets as comparable as possible. The exposure calculations use the population data from 2019 also for the scenario year 2030 for comparison reasons.

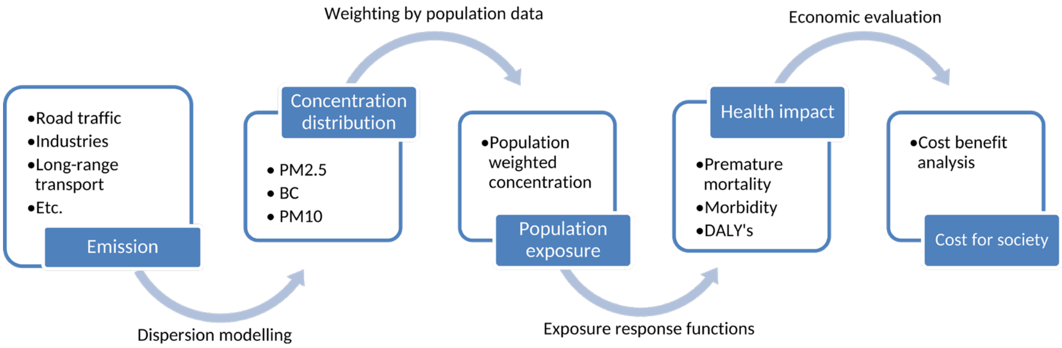

Figure 1. Steps involved in calculation of health impact and costs following the impact pathway (image from Segersson, 2021).

3.1 Emission data

Dispersion models require emissions as input data. Gridded emissions (1x1 km^2 resolution) within Sweden have been prepared by SMED[3] for 2019, as well as for two scenarios for year 2030, named “reference”[4] and “alternative”.

The assumptions for road emissions for the two scenarios for 2030 are described in Hult et al. (2022). Table 1 (Hult et al. 2022) describes the difference in assumptions for road traffic between the “reference scenario 2020” (our reference scenario) and the “EU regulations scenario” (used in our alternative scenario). The EU regulations scenario include:

- the assumptions from the “reference scenario 2020”,
- the greenhouse gas reduction mandate,
- model updates,
- higher rate of electrification,
- lower efficiency rate for combustion engines and more strict EU CO2 regulations.

[3] Geographically distributed emission data from SMED (emission year 2019): https://www.smhi.se/data/miljo/nationella-emissionsdatabasen

[4] Emission data reported to the EU in March 2021.

For example, the number of newly registered fully electric cars in 2030 is 18% in the reference scenario[5] and 68% in the EU regulations scenario[6].

In regards to other emission sectors, the alternative scenario includes

- a decrease in NO_x emissions from public electricity and heat production by 2 kton by 2030 compared to the reference scenario.
- a decrease in NO_x emissions from industrial combustion plants (the pulp and paper industry) by 3.6 ktons by 2030 compared to the reference scenario[7].

Emissions from the rest of Europe are based on different data sources for 2019 and 2030. For 2019, EMEP emissions[8] are used (0.1 degree resolution), while for 2030, the emission scenario ECLIPSE V6b[9] is used (0.5 degree resolution). ECLIPSE data is used for example in the GAINS model and include assumptions in line with the revised EU NEC Directive. A special delivery of ECLIPSE data was used, which excluded Swedish emissions, thus allowing combination with the prepared SMED emission data described above.

Emissions from forest fires are also included in the European model calculation, in the form of daily data from CAMS Global Fire Assimilation System (CAMS-GFAS). These emissions are equal for 2019 and the two 2030 scenarios.

Using two different sources of European emission data for 2019 and 2030 is not ideal, as there are differences in methodology and resolution, which affect the comparison between the results. EMEP emissions for 2019 are of high quality and relatively high resolution. Unfortunately, there is no geographically distributed emission scenario for 2030 from EMEP. ECLIPSE, on the other hand, has emission data for both 2019 and 2030, but at a much coarser resolution. We decided to use EMEP for 2019, in order to create the best possible assessment for the baseline year. Scenario years are in multiple ways connected to further uncertainties (both in emission levels and spatial distribution), and ECLIPSE emission data is regarded as the best choice for 2030.

3.1.1 Further improved urban emissions

In order to allow higher spatial resolution than 1x1 km^2 for the urban dispersion modelling, the gridded emissions from SMED were improved by using more detailed representations for road traffic, large point-sources and for small-scale residential heating.

High resolution emissions from small-scale residential heating have been attained by a method that combines data from the chimney sweeps records, the property register and fuel statistics from the Swedish Energy Agency. These emissions are scaled regionally with regional total emissions from SMED in order to fully comply with national statistics.

---

[5] Table 5 in SMED PM (https://admin.smed.se/app/uploads/2021/01/SMED-PM_NOx-i-klimatscenarier-f%C3%B6r-v%C3%A4gtrafik.pdf)

[6] Table 4 in Hult et al., 2022 (https://www.ivl.se/download/18.147c3211181202f18d1ec0b/1656151330841/C668.pdf).

[7] E-mail from Maria Ullerstam, Naturvårdsverket, 2021-12-13

[8] EMEP emission database (emission year 2019): https://www.ceip.at/webdab-emission-database

[9] ECLIPSE V6b global emissions from IIASA (emission year 2030): https://previous.iiasa.ac.at/web/home/research/researchPrograms/air/ECLIPSEv6b.html

Road emissions are calculated using the Swedish National Road Database[10], emission factors from HBEFA 4.1[11], together with fleet composition, and traffic flow as described by the air quality system SIMAIR[12] which is an application based on the CLAIR platform (see section 3.3.1). The road database contains for example traffic data such as annual average daily traffic, the fleet composition and usage of studded tyres in different regions in Sweden. An additional improvement was introduced for tunnels, approximating emissions at tunnel entrances and exits by emissions generated inside the tunnel (emissions from the first 300m in the tunnel are moved to the tunnel entrance, in both ends). Hourly exhaust and non-exhaust emissions are calculated for each road.

The non-exhaust emissions from traffic are modelled using the emission model NORTRIP[13], which has recently been integrated into the CLAIR platform. This model is used to calculate non-exhaust emissions hour-by-hour and considers meteorological conditions such as humidity, precipitation, temperature etc in order to estimate direct emissions to the air, as well as emissions that are retained temporarily on the road, forming a dust layer that may be suspended later. The most important processes generating non-exhaust emissions from road traffic are road, brake and tyre wear. Where sanding is used during winter time, this constitutes an additional source. The size-distributions for PM generated by these different processes are prescribed in the NORTRIP model configuration (for the calculations in this project, the default size-distributions are used). When all different processes represented in NORTRIP are considered the fraction of PM2.5 in relation to PM10 is approximately 8%. This is a lower fraction than has been assumed in previous studies, resulting in lower emissions of non-exhaust PM2.5 in this study in comparison to other studies (e.g. Segersson et al. 2017).

For the 2030 scenarios, emission factors and fleet composition were adjusted according to the scenario assumptions. For small-scale residential heating, the emissions for 2019 were scaled to agree with the scenario emissions from SMED at 1x1 km^2 resolution, while maintaining a higher spatial resolution.

Changes between 2019 and 2030 that are considered by NORTRIP are: increase in traffic volume, changes in share of heavy vehicles and changes in share of studded tyres during winter time. Other changes between 2019 and 2030 are likely, but uncertain. The increased average weight of vehicles due to electrification is one such example. The relation between vehicle weight and non-exhaust emissions from e.g. road wear is not well known and not described by NORTRIP. Consequently, this aspect was not considered. Also, changes in road maintenance (sanding, salting, cleaning, ploughing and dust-binding) are not considered. For 2030, the share of studded tyres is in general lower than for 2019 (a decrease expected in southern Sweden of approximately 10-20 percentage points), which decreases the non-exhaust emissions. The overall increase in traffic volume on the other hand (by approximately 10%), increases the emissions, especially if there is also an increased share of heavy vehicles (a slight increase expected by 2030 by approximately 1 percentage point). No detailed analysis was performed regarding how the different processes generating non-exhaust emissions change in the

---

[10] Swedish National Road Database: https://www.nvdb.se/sv/about-nvdb/

[11] HBEFA: https://www.hbefa.net/e/index.html

[12] Technical documentation of SIMAIR: https://www.smhi.se/forskning/forskningsenheter/luftmiljo/simair-teknisk-beskrivning-1.602

[13] NORTRIP: https://www.nilu.no/wp-content/uploads/dnn/23-2012-BDE-IS_NORTRIP-model-description.pdf

future scenarios. Also, since emission calculations were performed for individual roads in parallel with the dispersion modelling, no total national emission for non-exhaust emissions is presented.

In the following diagrams (Figure 2) Swedish emissions are presented for 2019 and the two scenarios for 2030. The different emission sectors are defined according to the GNFR activity categories[14] which are presented in Table 1. Note that non-exhaust traffic emissions are not included in the diagrams, because emissions are calculated dynamically within the dispersion modelling calculations.

In Table 2 total emissions for 2019 and the two emission scenarios for 2030 are presented, and the emission reduction compared to 2019 and compared to the reference scenario 2030 is calculated.

Table 1. GNFR emission sectors and descriptions.

GNFR	Description
A: PublicPower	Emissions from public electricity and heat production
B: Industry	Emissions from industrial combustion plants
C: OtherStationaryComb	Emissions from small combustion plants
D: Fugitive	Fugitive emissions
E: Solvents	Emissions from the use of solvents
F: RoadTransport	Emissions from road transport
G: Shipping	Emissions from domestic shipping
H: Aviation	Emissions from landing and take-off, for domestic and international flights
I: Offroad	Emissions from offroad mobility, such as machinery used in industry, households, agriculture, railways and fishing.
J: Waste	Emissions associated with waste handling (except combustion for energy).
K: AgriLivestock	Emissions associated with livestock and manure management
L: AgriOther	All other agricultural emissions, such as fertilizer, crops and field management
M: Other	Other anthropogenic sources
N: Natural	Emissions from natural sources, such as forest fires.

[14] GNFR activity codes: https://www.ceip.at/fileadmin/inhalte/ceip/1_reporting_guidelines2014/annex_i_rev18-11.xlsx

O: AviCruise	Emissions from the cruise phase of both domestic and international flights
P: IntShipping	Emissions from international shipping.
z_Memo	Multilateral operations

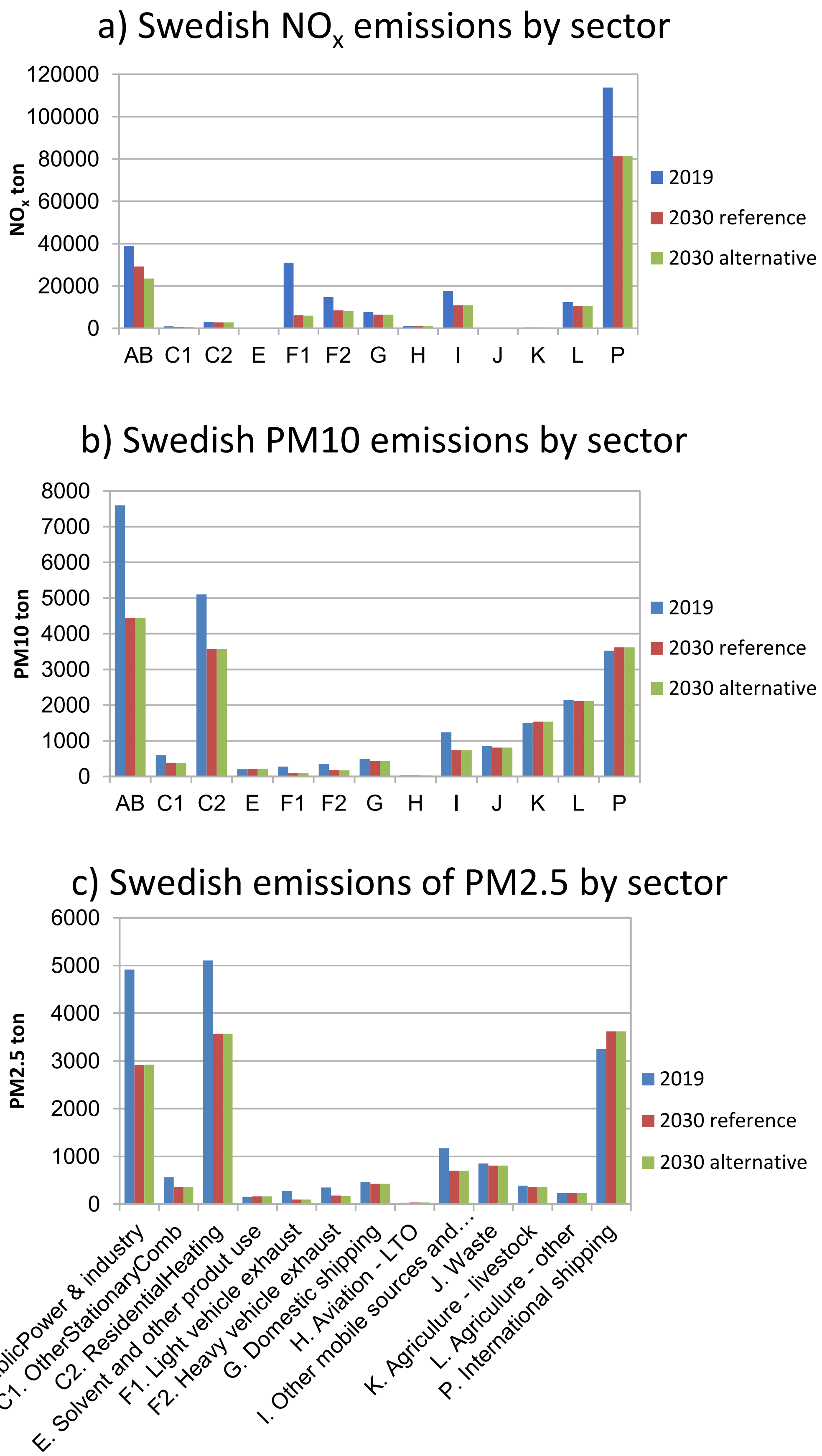

Figure 2. Swedish emissions by sector for 2019, 2030 reference scenario and 2030 alternative scenario for a) NO_x, b) PM10 and c) PM2.5.

Table 2. Swedish emissions for 2019 and the two scenarios for 2030.

Pollutant	**NO_x**			**PM10**			**PM2.5**		
Year/scenario	2019	2030 ref	2030 alt	2019	2030 ref	2030 alt	2019	2030 ref	2030 alt
Total emission (ton)	241 829	158 160	151 972	23 907*	18 159 *	18 147 *	17 736*	13 448 *	13 445 *
Reduction compared to 2019		34.6%	37.2%		24.0% *	24.1% *		24.2% *	24.2% *
Reduction compared to 2030 reference			3.9%			0.1%			0.0%

* Note that non-exhaust traffic emissions are not included.

In Figure 3 to Figure 8 some examples of emission data are visualized, for road emissions, small-scale residential heating emissions and shipping emissions.

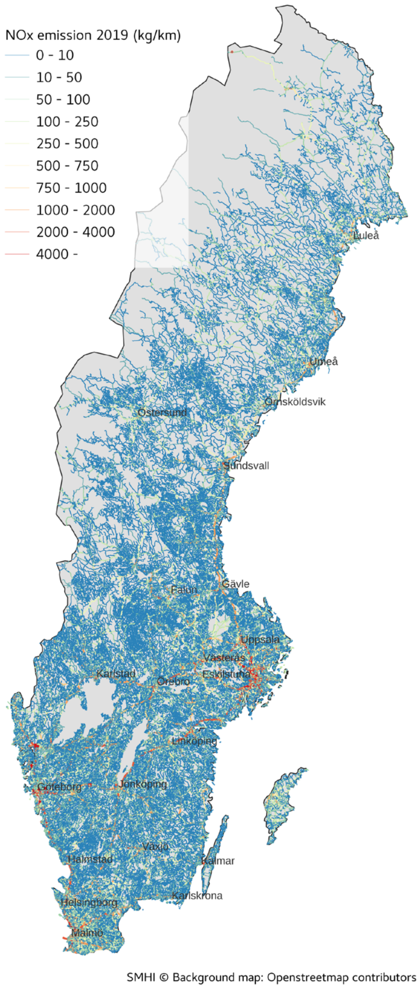

Figure 3. Road emissions of NO_x for 2019 for Sweden.

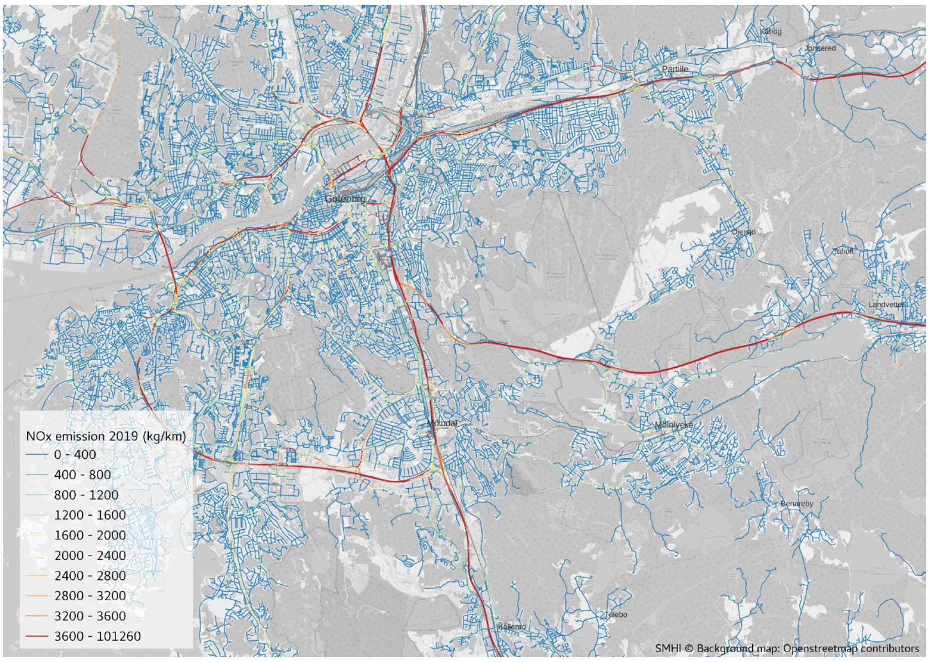

Figure 4. Road emissions of NO_x for 2019 zoomed in over Gothenburg. The emissions are line sources along the Swedish national road database.

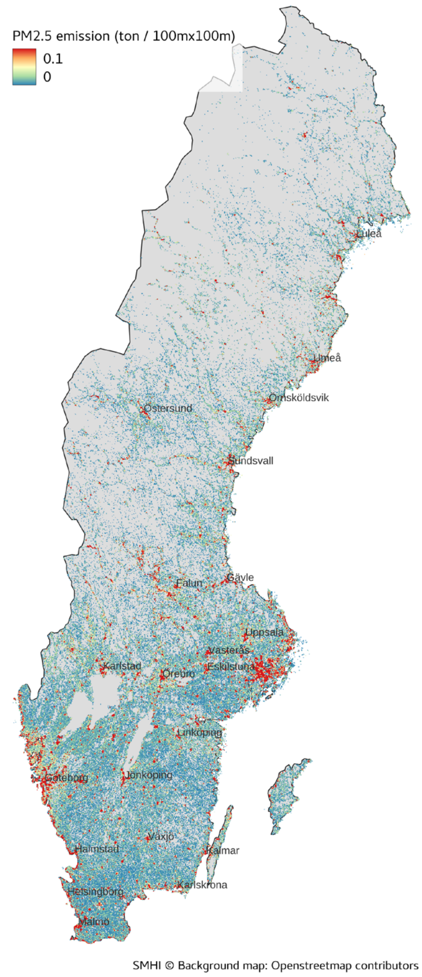

Figure 5. Emissions of PM2.5 from small-scale residential heating for 2019 over Sweden.

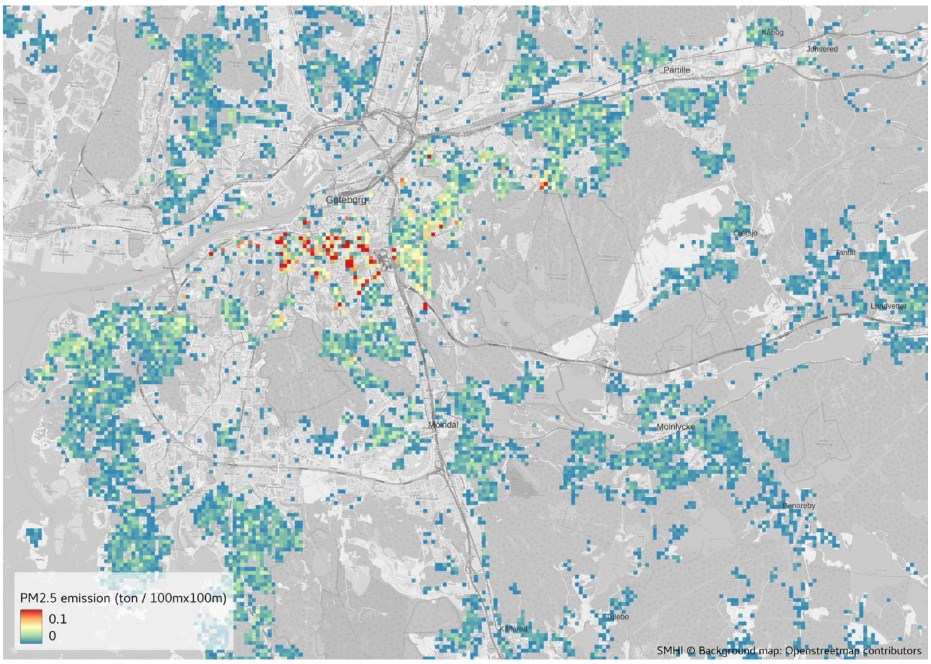

Figure 6. Emissions of PM2.5 from small-scale residential heating for 2019 zoomed in over Gothenburg. The emission data has a resolution of 100 m.

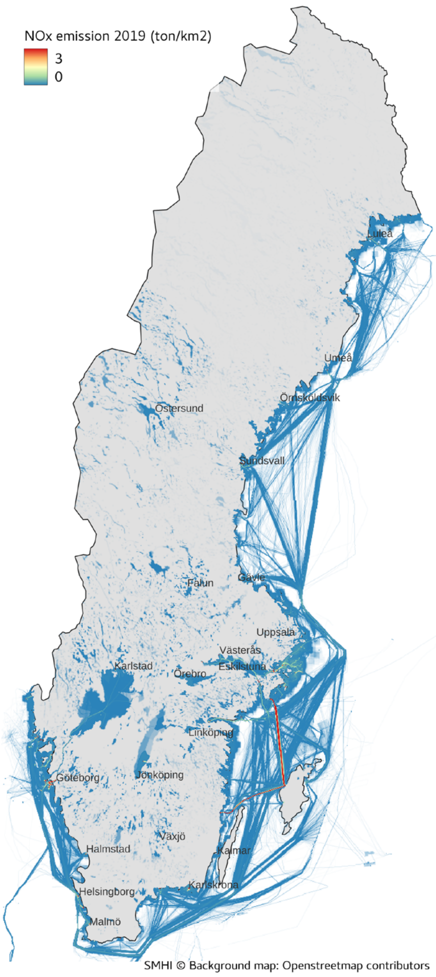

Figure 7. Domestic civil shipping emissions of NO_x for Sweden for 2019.

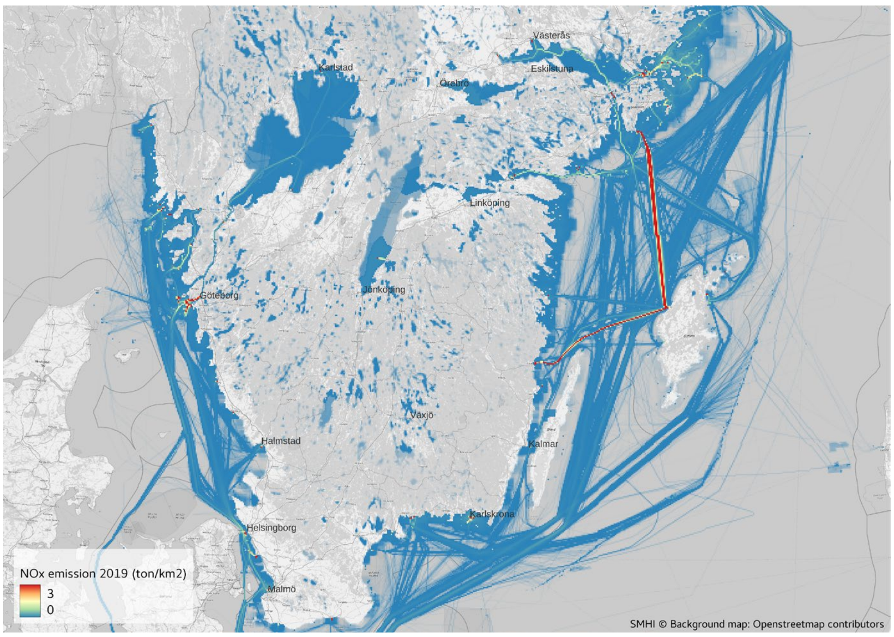

Figure 8. Domestic civil shipping emissions of NO_x for 2019 zoomed in over the southeast Swedish coast. The emission pattern is based on the SMHI emission model Shipair.

3.2 Meteorological data

The meteorology data that is used in the model runs are gridded data for 2019. In the MATCH model, 3-dimensional meteorological data for all of Europe is needed and data from the ECMWF weather model HRES[15] (0.1 degree resolution) is used. For the urban dispersion modelling, hourly weather data from MESAN[16] (2.5 km resolution) is used, together with global radiation from STRÅNG[17].

The meteorology varies from one year to the next, which can cause variations in air pollution concentrations and in e.g. precipitation. Generally, cold and stable weather tends to create atmospheric conditions which promote high air pollution levels while wet and windy weather tend to have a decreasing effect on air pollution levels. Emissions from natural sources vary with the meteorology but the anthropogenic emissions usually vary less between each year.

The year of 2019 was a warm and wet year[18] compared to the 30-year period of 1961-1990, which is the standard normal period decided by the World Meteorological Organization. The warm weather, not only in Sweden but in all of Europe, has effects on for example ozone and particulate matter. Warm and sunny weather in the summer months increases ozone production. Warm weather in the winter months decreases the amount of PM emissions from small-scale heating, thus also likely has a reducing effect on the concentration levels of particles.

In Figure 9 the temperature and precipitation deviation of 2019 from the normal period is shown for Sweden.

---

[15] HRES meteorological data: https://confluence.ecmwf.int/display/FUG/HRES+-+High-Resolution+Forecast

[16] MESAN meteorological data: https://www.smhi.se/data/utforskaren-oppna-data/meteorologisk-analysmodell-mesan-arome-api

[17] STRÅNG global radiation data: https://www.smhi.se/forskning/forskningsenheter/atmosfarisk-fjarranalys/strang-en-modell-for-solstralning-1.329

[18] SMHI: https://www.smhi.se/klimat/2.1199/aret-2019-varmt-och-blott-1.154497

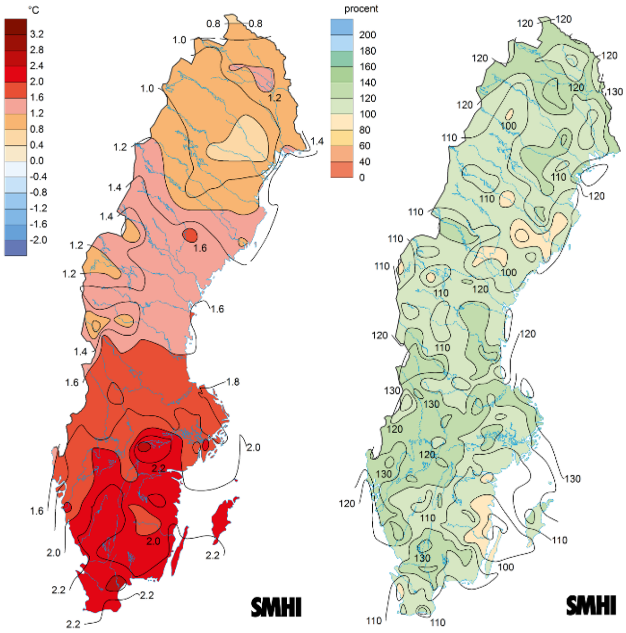

Figure 9. Annual mean deviations in temperature (˚C) and precipitation (percent) from the normal annual mean (mean value of 1961-1990) for 2019.

3.3 Dispersion calculations

3.3.1 The CLAIR platform

In recent years, SMHI has built a new air quality modelling toolbox called CLAIR, which features urban and local dispersion models downscaling modelled regional scale concentrations of air pollutants, integrated with bottom-up national emission inventories and models as well as monitoring data.

The CLAIR platform allows parallel execution of urban and/or local scale dispersion models. CLAIR includes tools to perform modelling using a tiled approach, where urban scale dispersion modelling is performed for multiple small areas (around 10x10 km^2) and then aggregated to produce a complete dataset (Segersson et al., 2021). This allows for very high-resolution model results across the whole of Sweden.

The modelling toolbox has undergone thorough evaluations and has been applied for multi-year exposure simulations regionally and nationally for Sweden aimed at developing new dose-response functions for health impacts and serves as a core component in a range of on-going research projects and air quality services currently provided at SMHI.

3.3.2 The modelling concept

A combination of dispersion modelling at regional and urban scale has been used, where transport over longer distances than around 15 km is described by the regional dispersion model MATCH (Multi-scale Atmospheric Transport and CHemistry model) (Robertson et al., 1999; Andersson et al., 2007; Andersson et al., 2014) and transport at shorter distances is described using the Gaussian model NG2M which is run on the CLAIR platform. Each model is tailored to capture the most important processes at the spatial and temporal scale for which they are applied.

In order to avoid double-counting contributions from sources when adding concentrations from the regional and the urban dispersion model, the contribution from local sources is first removed from the regional concentration fields. This is handled by a post-processing scheme named BUDD (Backtrace Upwind Diffuse Downwind). BUDD follows a trajectory upstream to find the concentration unaffected by nearby emissions. A vertical profile at the upstream location is then allowed to diffuse while travelling downstream, ensuring that high-level emissions at the upstream location are not neglected.

The full modelling concept is further described in Segersson et al. (2021). In Figure 10 the concept is presented in a schematic diagram.

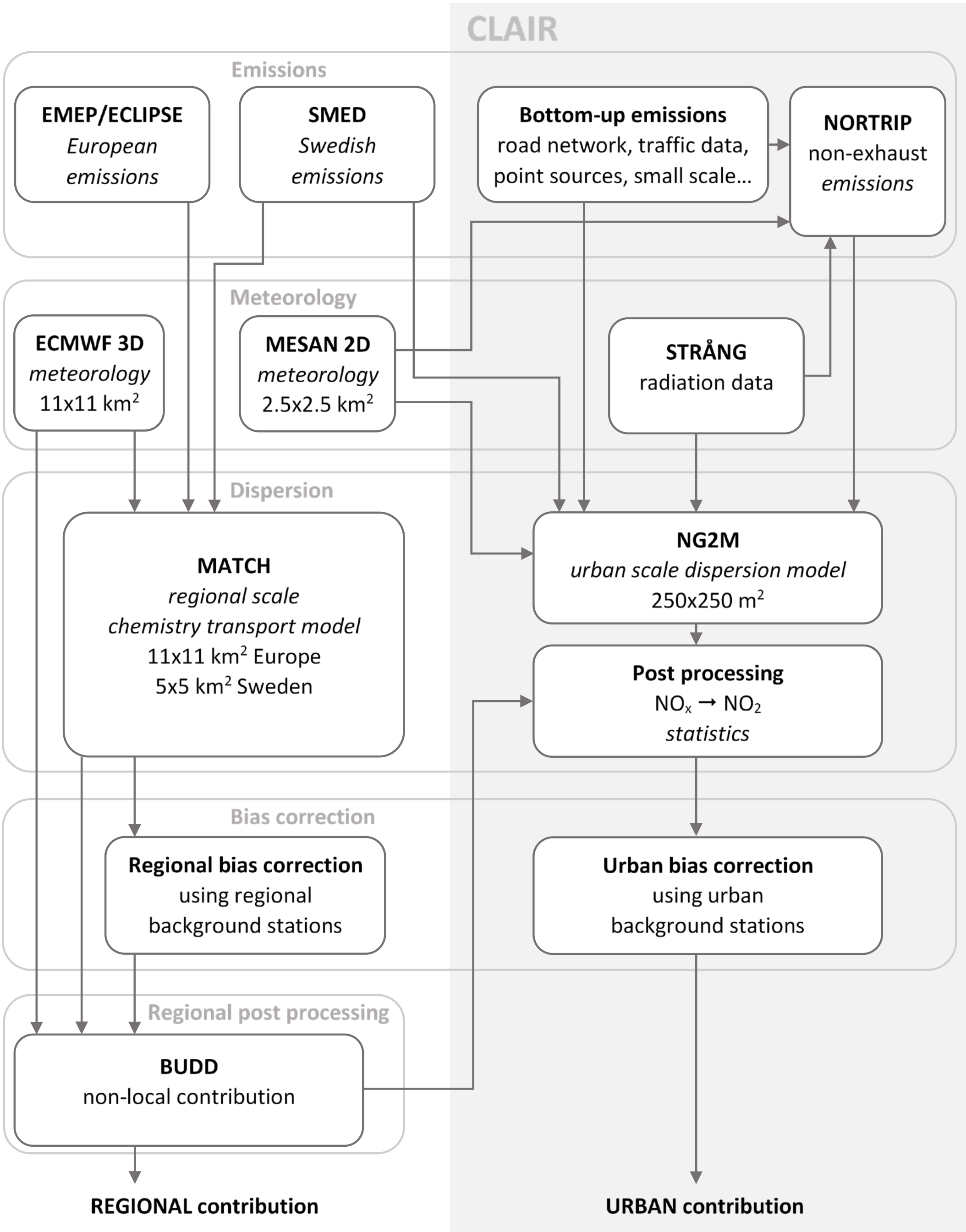

Figure 10. Schematic presentation of the modelling concept used in this study.

3.3.3 Regional scale dispersion calculations

The chemical transport model MATCH is used to calculate the regional concentration levels at a 5 km horizontal resolution. A model run is first carried out for all of Europe on 0.1 degree resolution (approximately 11 km). A nested model approach is used to further increase spatial resolution over Sweden to 5 km. Results from the coarser model run is used as boundary conditions. This method allows for MATCH to capture contributions from the entire European continent, and have higher resolution over Sweden, despite very heavy MATCH calculations on a supercomputing cluster at the National Supercomputer Centre (NSC) in Linköping.

Emissions from forest fires are included in the European model calculation, in the form of daily data from CAMS Global Fire Assimilation System (CAMS-GFAS). Sea salt contribution to particulate matter is also included in the MATCH calculation.

There are particle emission sources that are diffuse and difficult to describe; for example dust from agriculture, pollen and other natural sources; which are partly or totally missing in the emission data used in this modelling. In order to avoid systematic underestimation of modelled particle levels, a bias-correction is carried out using hourly/daily regional measurement data for 2019. The daily bias is calculated at the location of each regional background measurement site, and an interpolation is then carried out hour by hour over Sweden, where the delta is used to adjust the modelled concentration fields.

A similar approach is used for regional measurements of NO_2 and O_3, in order to create the most accurate regional background concentrations for 2019.

For the scenarios of 2030, the same measurement adjustments are used as for 2019, for particulate matter. It is assumed that the delta seen in regional background is mainly caused by (primarily natural) emissions that are not included in the emission inventories. These emissions are thought to be missing for 2030 as well, which motivates the same delta as for 2019.

Finally, the post-processing scheme named BUDD (Backtrace Upwind Diffuse Downwind) is applied to the regional concentrations in order to not double count contributions from urban sources.

3.3.4 Urban scale dispersion modelling

An urban contribution to the pollution concentration levels at a 250 m resolution is then calculated using the modelling toolbox CLAIR, with the Gaussian dispersion model NG2M.

In order to efficiently run the NG2M dispersion model, the national domain is divided into sub-domains here called tiles. Each tile is 10x10 km large and corresponds to a model run. For each tile, emission sources within the tile and an emission buffer zone are included in the simulation. The horizontal resolution is 250 meters, which means that each tile contains 40x40=1600 receptor points.

Within the modelling domain, the urban scale dispersion modelling has been limited to all (10x10 km^2) tiles where at least one person lives, leading to 3738 tiles in total, which in turn means that concentrations have been calculated at almost 6 million receptor points. For the tiles where there is no population, the regional scale modelling results have been used instead, in order to obtain a full result.

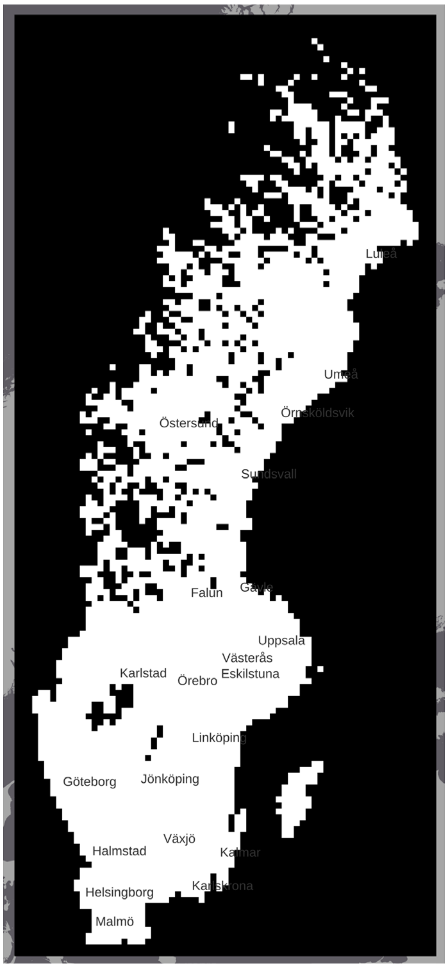

Figure 11. The tiles (sub-domains) where urban scale dispersion modelling has been carried out can be seen in the map (white cells). For black cells, no urban-scale modelling is run and the concentrations are only described using the regional scale dispersion model.

The dispersion simulations are run hour-by-hour, using hourly meteorological input, hourly emission data and also hourly data for regional background concentrations.

To provide a source apportionment, five emission sectors are handled separately in the NG2M model. The following sectors have been used in the project (see Table 1 for information on GNFR sectors):

- Traffic exhaust: GNFR sector F (excluding tyre and brake wear, road abrasion)
- Traffic non-exhaust: non-exhaust calculated using NORTRIP
- Small-scale residential heating: GNFR sector C2
- Shipping: GNFR sectors G, P
- Other sources: GNFR sectors A, B, C1, E, H, I, J, K, L

The different sectors are treated as different source types in the NG2M dispersion model. Traffic sources are line sources for each road segment and small-scale heating are gridded sources at 100 m resolution. Shipping emissions are also treated as gridded emission sources, while the “other sources” sector contains a mixture of gridded emissions and discrete point sources for large industrial facilities. The NG2M model point sources to include effects of plume-rise and downdraft. Gridded emissions may have different release heights for different sectors.

While the CLAIR system runs on a server at SMHI, the NG2M dispersion model is executed remotely on a supercomputing cluster at the National Supercomputer Centre (NSC) in Linköping. Multiple tiles are run in parallel, and within each tile the NG2M model is parallelized in time and for substances, allowing for all pollutants to be modeled in the same run.

In order to model NO_2, the CLAIR system first models NO_x, then postprocesses the hourly NO_x results to obtain NO_2 and O_3, assuming pseudo steady-state (Berkowicz et al., 2011). The postprocessing is performed on the same resolution as the NG2M dispersion model results and the regional background is interpolated to match the local grid.

As a final step in the simulation in each tile, relevant statistical metrics are calculated, such as yearly means and percentiles relevant to each substance modelled.

Finally, using hourly/daily urban background measurements, a correction is carried out based on the bias at each measurement site. Correction factors are gradually dampened with distance from the measurement site. At distances longer than 30 km there is no influence from an urban monitoring station.

All available hourly and daily measurements with enough data availability (minimum 75%) in urban background are used for PM10, PM2.5 and NO_2. Scaling is done on the annual mean and on percentiles. The scaling factor is applied equally to all source contributions. The urban scaling is applied to the 2030 scenarios as well in order to improve comparability between the years.

A validation of model results compared to urban background measurements is carried out for 2019 and presented in section 4.4, in order to ensure sufficient model quality.

3.4 Exposure calculations

In order to do exposure calculations, spatial population data is needed. In this project, data from Statistics Sweden is used, which includes gridded number of inhabitants at 250x250 m^2 grids within urban areas and 1x1 km^2 grids outside urban areas. The population data is divided into the age categories 0-15, 16-20, 21-30, 31- 50, 51-65 and above 65 years. Population data is from the register of total population 2019-12-31.

For the annual average concentrations of PM10, PM2.5 and NO_2, population exposure is calculated for each age category as well as for the total population. Exposure is calculated for the total concentrations, but also divided into a regional and an urban contribution. For PM, which is treated as inert in the urban dispersion modelling, the urban contribution is further divided into source specific contributions from small-scale residential heating, shipping, road traffic (exhaust), road traffic (non-exhaust) and other sources.

3.5 Health impact assessment

3.5.1 Estimation principles and components

Health impact assessments (HIAs) are built on epidemiological findings; exposure-response functions (ERFs) and population relevant rates describing how frequent the health outcome is. A typical ERF shows how the relative risk changes with the exposure. The common health impact calculation has four components: a relevant epidemiological ERF, a baseline rate for the health outcome in the studied population, the number of persons exposed and their estimated “exposure” (here pollutant concentration).

The excess number of cases per year has been calculated as:

$$\Delta y = (y_0 \bullet pop)\,(e^{ß \bullet \Delta x} - 1)$$

where y_0 is the baseline rate, pop is the affected number of persons; ß is the exposure-response function (natural logarithm of relative risk (RR) per change in concentration), and x is the estimated (excess) exposure (WHO, 2016b).

Information on the population number and age distribution in different geographical areas, as well as the base-line rates in the country or region, can often be obtained from registers or official statistics and could then be seen as objective facts. The exposure data can originate from different monitoring or modelling methods with potential differences also in spatial and temporal resolution, which could result in differences in exposure estimates even for the same case or scenario. The probably most important and complicated reason for potential differences in the estimated health impacts is the assumed exposure-response function for the specific exposure, the slope and if there is a lower threshold below which no association exists. Epidemiological studies, and also wider literature reviews with a meta-analysis, may produce quite different exposure-response functions as result of the included data, or for different study locations and concentration ranges.

Another complicated question in an HIA is how to deal with correlated exposures, for example fine particles (usually measured as PM2.5) and NO_2. When the ERF comes from a single-pollutant model it is not adjusted for the potential effect of any other pollutant. In such a case, the ERF for PM2.5 may partly be driven by effects from the positive correlation with NO_2 and vice versa. If the health impacts are calculated separately from both pollutants this may cause an overestimation (“double counting”) of the burden. If instead only one of two pollutants with causal effects is studied, this would lead to an underestimation of their total health impacts. In some HIAs this has motivated the use of ERFs from a multiple-pollutant model. Another pragmatic solution has been to reduce one of the ERFs by a certain percent.

The impact of PM2.5 on premature mortality, sometimes expressed as years of life lost, has been the major health effect of air pollution exposure in almost all health impact assessments regardless of if the national or global burden was estimated. The established association between particle exposure and mortality continues to be the major air pollution related health problem according also to the new WHO Air Quality Guidelines (WHO, 2021). During the more than 15 years that have passed between the last and new air quality guidelines, new studies have reported adverse effects at much lower levels than previously reported, which has resulted in more strict guidelines. Moreover, recent studies of mortality with rather low concentrations of PM2.5 have reported higher relative risks per unit increase in concentration (steeper increase), especially for PM2.5 from local sources (Segersson et al, 2021).

Air pollution exposure is however not only associated with mortality, but also associated with a considerable burden of disease related to morbidity effects, as shown by the

Global Burdens of Disease Project (GBD 2019 Collaborators, 2020). In the past, most health impact calculations focused on the effects of short-term exposure on short-term effects such as the daily number of hospital admissions, based on results from time-series studies. More recently the focus has changed towards estimation of the impact on the incidence of chronic diseases, based on ERFs from cohort studies.

As one of the aims of this study according to Naturvårdsverket (Swedish EPA) has been to compare the results with the population exposure modelled for 2019 in this study with the reported results for 2019 obtained in a parallel study using different methods to calculate the population exposure, the core health impact calculations are made by the same author (BF) with the same ERFs and baseline rates as were selected for the parallel study (Gustavsson et al, 2022). For this reason, the two following sections on ERFs and baseline rates (3.5.2 and 3.5.3) are almost identical with the corresponding sections in the previous report (Gustavsson et al, 2022). In addition, some sensitivity analyses have been included when motivated by reports published 2022.

3.5.2 Mortality

Fine particles have different origin, composition and properties in different places. Particles may be primary or secondary, natural or anthropogenic, and consist more or less from minerals, soot, metals, salts etcetera. Thus, depending on the location, spatial resolution and the particle exposure variables, studies have a different potential to reflect the association between a specific type of exposure and mortality.

A systematic review of the evidence of associations between long-term exposure to particulate matter (PM2.5 and PM10) was recently published with the objective to support the new WHO Air Quality Guidelines (Chen & Hoek, 2020). For natural-cause mortality, the combined effect estimate across 25 studies was 1.08 (95% CI 1.06 - 1.09) per 10 µg/m^3. The authors comment that "the large heterogeneity of effect estimates across studies suggests that health impact assessments in specific locations may have fairly large uncertainty". Notable, for the five studies with the lowest mean concentration, all below 10 µg/m^3 and relevant for Sweden, the combined effect estimate was more than doubled, 1.17 per 10 µg/m^3 (95% CI 1.12 - 1.23). This higher relative risk could perhaps be a result of less variation in exposure explained by the regional background in the underlying studies, and more variation in exposure related to local sources and within-city patterns.

A recent Swedish health impact assessment questions the use of the same exposure-response function for PM2.5 and mortality regardless of the exposure level (Segersson et al, 2021). It is now well documented that the increase in risk per µg/m^3 is bigger at low total PM2.5 concentrations and for the local sources such as traffic, than for the regional background of PM2.5. It has been shown, even within large cohort studies, that the scale of spatial variability in concentrations is important for the estimated increase in mortality per µg/m^3 (Segersson et al, 2021). Turner et al (2016) in their multiple pollution model observed a more than six times higher relative risk (1.26 per 10 µg/m^3) per absolute increase in concentration for near-source PM2.5 in comparison with regional PM2.5 (1.04 per 10 µg/m^3). Lefler et al (2019) found similar patterns and concluded that regressions using spatially decomposed PM2.5 suggest that more spatially variable components of PM2.5 may be more toxic. An important review used meta-regression techniques to test whether study population or analytic characteristics modify the PM2.5 -mortality association and to estimate the shape of the concentration-response curve (Vodonos et al, 2018). The authors found the PM2.5 coefficient to decrease inversely proportional to the mean concentration. For all-cause all-age mortality, a 1 µg/m^3 increase in PM2.5 was associated with a 1.29% increase in all-age all-cause mortality at a mean exposure of 10 µg/m^3, which decreased to 1.03% at a mean exposure of 15.7 µg/m^3 (the mean level across all studies). Restricted to studies with mean PM2.5 concentrations below 10 µg/m^3, the increase was 2.4% (95% CI 0.8 - 4.0) increase per 1 µg/m^3.

A study of the Canadian community health survey cohort (Pinault et al, 2016) is interesting because of the low PM2.5 concentrations with a mean = 6.3 µg/m^3 and the detailed data on life style. For non-accidental mortality, the relative risk was 1.26 (95% CI: 1.19 - 1.34) per 10 µg/m^3, and although the lowest measured concentration of PM2.5 was 1 µg/m^3, the authors found no lower threshold for response.

A new important European study is the pooled analysis of eight cohorts in the multi-centre project Effects of Low-Level Air Pollution: A Study in Europe (ELAPSE). In this study 325 367 adults were followed-up for an average of 19.5 years, with 47 131 observed deaths. An increase of 5 µg/m^3 in PM2.5 was associated with 13% (95% CI 10.6 - 15.5) increase in natural deaths (Strak et al, 2021). Associations tended to be steeper at low concentrations, levelling off at high concentrations. For participants with exposures below the US standard of 12 µg/m^3 an increase of 5 µg/m^3 in PM2.5 was associated with 29.6% (95% CI 14% - 47.4%) increase in natural deaths.

A recent Swedish multi-cohort study within the Swedish Clean Air and Climate Research Program (SCAC) high-resolution dispersion models were used to estimate annual mean concentrations of PM10, PM2.5 and BC at individual addresses during each year of follow-up, 1990-2011 (Nilsson Sommar et al, 2021). Moving averages were calculated for the time windows 1-5 years (lag1-5) and 6-10 years (lag6-10) preceding the outcome. For PM2.5 (range: 4.0 - 22.4 µg/m^3), the estimated increase in SCAC was 13% per 5 µg/m^3, as in a Danish cohort (Hvidfeldt et al, 2019) and the European multi-cohort study ELAPSE (Strak et al, 2021), but less precise (95% CI -9 - 40%). However, for cardiovascular mortality the increase in SCAC was bigger and statistically significant, 23% per 5 µg/m^3 PM2.5 (95% CI 3 - 48) for lag 1–5 years.

Since a large part of PM10 is PM2.5, and the finer fraction generally is found to be more toxic, it is not possible to estimate the long-term effects on mortality of both PM2.5 and PM10 as they were independent, even if some relative risks associated with PM10 exposure have been published.

A systematic review of the evidence of associations between long-term exposure to NO_2 and mortality was recently published with the objective to support the new WHO Air Quality Guidelines (Huangfu & Atkinson, 2020). For natural-cause mortality, the combined effect estimate across 24 studies was 1.02 (95% CI 1.01 - 1.04) per 10 µg/m^3. In this case the evidence was considered moderate, but this estimate from single pollutant models was used as basis for the guideline development (WHO, 2021). However, associations between NO_2 and mortality have been sensitive to adjustment for particles. Results from multiple pollution models report relative risks more in line with the lower end of the 95% CI from Huangfu & Atkinson (Turner et al, 2016; Stieb et al, 2021).

Assumed functions and baseline for mortality

Recent studies investigating the associations between the local variation in long-term levels of PM2.5 and mortality in adult cohorts consistently find much higher relative risks than typical when all types of studies are considered. High meta estimates are also obtained when results from studies with low levels are combined, but this is likely because these results are more than other studies influenced by local sources and contrasts within cities, and less by variation in the regional background concentrations.

As the most relevant relative risk assumption for local sources, traffic and domestic wood burning, we see the original results reported by Turner et al. (2016), Pinault et al. (2016), Hvidfeldt et al. (2019), Strak et al. (2021) and Nilsson Sommar et al. (2021), which also were supported by the analyses by Vodonos et al. (2018) and Lefler et al. (2019). We here apply a relative risk of 1.26 per 10 µg/m^3, and 95 % confidence limits from Turner et al (2016).

For the effect on mortality from the regional background concentration of PM2.5, mainly long-distance transported particles, and for the urban contribution of NO_2 we apply the overall relative risks assumed in the WHO Air Quality Guidelines (WHO, 2021): 1.08 and 1.02, respectively per 10 µg/m^3. Given the low regional background levels of NO_2 in Sweden in relation to levels in the epidemiological studies, and the before commonly assumed thresholds, no impacts are assumed from the regional background of NO_2.

The cited studies of long-term exposure and mortality all include only adults, typically 30 years or older when the follow up started. We here estimate the effect of long-term exposure on persons older than 30 years. Statistics from The National Board for Health and Welfare (Socialstyrelsen) reported for Sweden 2019 a total mortality of 1338 deaths per 100 000 persons in the age group 30+ based on data from the national Cause of Death Register[19].

3.5.3 Morbidity

According to international scientist's air pollution increases morbidity from a wide range of diseases (Thurston et al., 2017; Schaffer et al., 2019, Perera et al., 2019). According to WHO there is strong evidence for ischemic heart disease, stroke, chronic obstructive pulmonary disease (COPD), lung cancer and acute respiratory infections, and a growing body of evidence suggesting causal relationships for type II diabetes, short gestation and low birth weight and neurological diseases (WHO, 2021). Besides the trend of a growing list of morbidity outcomes associated with air pollutants, especially PM2.5, the strength of evidence is judged a bit different by different experts and organizations.

Since a large part of PM10 is PM2.5, and the finer fraction generally is found to be more toxic, it is as for mortality not possible to estimate the long-term effects on morbidity of both PM2.5 and PM10 as they were independent, even if some relative risks associated with PM10 exposure have been published.

Selected exposure-response functions and baselines for morbidity

In this health impact assessment we also for morbidity apply the same ERFs and baseline rates as were selected for the parallel Swedish study (Gustavsson et al, 2022). These outcomes and relative risk functions were selected after a literature review initiated by the Swedish Transport Administration for health cost calculations related to local emissions from road traffic (Söderkvist et al., 2019; Forsberg et al., 2021), except for stroke where we apply the relative risk from a more recent European multi-cohort study (Wolf et al, 2021). These relative risks were recommended to apply when the impact of local PM2.5 emissions is studied, which usually means exposures upon a regional background. Because most morbidity studies build on within-city variations in exposure and the lower side of the exposure range usually is above 5 µg/m^3, these risk estimates

[19] Cause of Death Register: https://www.socialstyrelsen.se/statistik-och-data/statistik/statistikdatabasen/

have not in HIAs been used for concentrations below new WHO Air Quality Guideline for PM2.5 of 5 µg/m^3 as annual mean. The same restriction was used in the parallel study and thus also in this study.

We have not judged it possible to also calculate corresponding health impacts related to NO_2 itself because of the correlation between the pollutants and lack of adjusted risk estimates.

The selected risk estimates are listed in Table 3 together with the corresponding baseline frequencies that are applied. National health register data were obtained from The National Board for Health and Welfare[20] (Socialstyrelsen) and the frequency usually represents 2017. For all diseases except childhood asthma the baseline frequency is calculated for incident (new) cases. For preterm birth and childhood asthma the baseline is estimated from prevalence data, the proportion of births that are preterm, and the proportion of persons with a persistent childhood asthma when they turn 20.

Table 3. Applied relative risks and the corresponding baseline frequencies.

Outcome/at risk	**RR from (source)***	**RR per 10 µg/m^3**	**% per 1**	**Freq/pers year**	**Freq from (source)***
Myocardial infarction/>30 yrs	Cesaroni G, 2014	1,12	1,1	0,00246	National health register
Stroke/>30 yrs	Wolf et al, 2021**	1,44	3,7	0,00253	National health register
Lung cancer/>30 yrs	Hvidtfelt U, 2021	1,28	2,5	0,00042	National health register
Dementia/>50 yrs	Yu X, 2020	1,17	1,6	0,00577	Van Bussel, 2017
Diabetes/>15 yrs	He D, 2017	1,25	2,3	0,00400	Norhammar, 2016
COPD/>50 yrs	Weichentahl S, 2017	1,20	1,8	0,00157	Lindberg, 2006
Childhood asthma/-20 yrs	Khreis H, 2017	1,34	3,0	0,07500	Oudin, 2017
Preterm birth	Klepac P, 2018	1,24	2,2	0,056***	National health register
*/ for details see Söderkvist et al. (2019) and Forsberg et al. (2021) ** <15 µg/m^3 ***/proportion of births					

[20] National health register: https://www.socialstyrelsen.se/statistik-och-data/statistik/statistikdatabasen/

The selection of risk functions takes into account how relevant and established the presented results are, where meta-estimates (from a literature review) and European multi-cohort results with relevant exposures were seen as a goal. European multi-cohort results are used for myocardial infarction (ESCAPE), stroke (ELAPSE) and lung cancer (ELAPSE). The relative risks applied for PM2.5 and diabetes, childhood asthma, dementia and preterm birth are all from review papers with a calculated meta-estimate. It is only for COPD the applied risk function comes from one single large study that was conducted in Toronto. The selection of these risk functions is further discussed in reports from the Swedish Transport Administration (Söderkvist et al., 2019; Forsberg et al., 2021).

3.5.4 Investigated sources and scenarios

This health impact assessment builds on the population exposure calculated in this study, and is organized to make it possible to add the impacts and still avoid double counting. Detailed calculations are undertaken for 2019 based on the collected population data and selected baselines. Relative changes associated with the 2030 scenarios are estimated.

Impact of regional background $PM_{2.5}$ on mortality

We estimate the impact of regional background $PM_{2.5}$ on all-cause mortality in persons older than 30 years of age and apply the overall relative risk assumed in the WHO Air Quality Guidelines (WHO, 2021) 1.08 per 10 µg/m^3. In lines with epidemiological results we assume no threshold below which the association not exists.

Impact of urban source $PM_{2.5}$ on mortality

We estimate the impact of PM2.5 from all studied urban sources on all-cause mortality in persons older than 30 years of age and apply a relative risk of 1.26 per 10 µg/m^3.

Impact of urban source NO_2 on mortality

We estimate an impact of NO_2 itself on all-cause mortality in persons older than 30 years of age without any specific cut off but only from the urban contribution. We apply the overall relative risks assumed in the WHO Air Quality Guidelines (WHO, 2021) 1.02 per 10 µg/m^3.

Impact of regional and urban PM on morbidity

We estimate the impact only of $PM_{2.5}$ on morbidity, applying the same risk functions regardless of type of particle source. For diseases and preterm birth, we use a cut off at 5 µg/m^3.

For restricted activity days the exposure-response relation we previously have applied is based on old cross-sectional and self-reported results from USA. This is a weak study design, but the results have been widely used, e.g. by WHO in HRAPIE (WHO, 2013a). Even if our previous calculations built on the total exposure range must be interpreted with caution, we in this assessment repeat the same type of estimation.

4 Results

4.1 Concentration levels

In the following subsections the annual mean concentrations of NO_2, PM10 and PM2.5 are presented for 2019 and 2030. For a selection of cities the source distribution is presented in diagrams.

4.1.1 Concentration levels compared to standards, objectives and guidelines

Modelled concentrations have been compared to the annual air quality standards, air quality objectives and the WHO revised guidelines, listed in Table 4. It should be noted that the model results represent urban background at a spatial resolution of 250 m, and are thus not comparable to local hotspot concentrations. There can be exceedances in for example street canyons that are not captured at the present resolution.

Table 4. The concentration levels corresponding to the air quality standards, air quality objectives and WHO guidelines for annual means of NO_2, PM10 and PM2.5 (unit µg/m^3).

Pollutant	**NO_2**	**PM10**	**PM2.5**
Air quality standard[21] (annual mean)	40	40	25
Air quality objective[22] (annual mean)	20	15	10
WHO guideline[23] (annual mean)	10	15	5

4.1.1.1 Exceedances during year 2019

During 2019, there are no exceedances of the annual air quality standard for NO_2 according to the model calculations, and only a few grid cells in Stockholm and Gothenburg with NO_2 values over the air quality objective of 20 µg/m^3. There are exceedances of the WHO guideline for NO_2 of 10 µg/m^3 in several cities, especially in the north of Sweden, as well as along major highways.

For PM10 there are no modelled exceedances of the air quality standard during 2019. There are however exceedances of the air quality objective (and the WHO guideline as

[21] The Swedish air quality standards: https://www.naturvardsverket.se/globalassets/vagledning/luft-och-klimat/mkn-utomhusluft/sammanstallning-miljokvalitetsnormer.pdf

[22] The Swedish environmental quality objectives for clean air: https://www.naturvardsverket.se/en/environmental-work/environmental-objectives/clean-air/

[23] WHO global air quality guidelines: https://apps.who.int/iris/bitstream/handle/10665/345329/9789240034228-eng.pdf?sequence=1&isAllowed=y

they are the same) in Gothenburg, Malmö and along the major highways, especially along the E6 from Kungälv and southwards and the E4 close to Stockholm.

For PM2.5 there are exceedances of the WHO guideline of 5 µg/m^3 for the south of Sweden, up to Gothenburg, Jönköping, Norrköping and Stockholm in 2019. Several medium sized cities further north, such as Uppsala, Västerås and Sundsvall also exceed the WHO guideline. There are no exceedances of the air quality objective nor the air quality standard for PM2.5 in 2019 according to the model calculations.

4.1.1.2 Exceedances in scenarios for year 2030

There are no annual exceedances of the air quality standards for NO_2 or PM10 in any of the 2030 scenarios (note that model results represent urban background, not local hotspots). For NO_2, compliance is achieved also for the air quality objectives, while for PM10 there are exceedances along major highways, mostly E4 and E6, as well as across a large part of Malmö. The two scenarios for 2030 show very similar results for PM10.

For NO_2, there are exceedances of the WHO guideline of 10 µg/m^3 in Gothenburg, outside Gällivare and at a few receptor points in Stockholm. A small decrease in NO_2 concentrations can be seen for the alternative scenario in comparison with the reference scenario, especially close to large industrial emission sources.

For PM2.5 for 2030 there is a small reduction in concentrations, resulting in levels below 5 µg/m^3 occurring slightly further south than for 2019. Several medium sized cities in mid Sweden no longer exceed the WHO guideline in 2030 according to the model results. In Figure 12 the annual mean concentrations for PM2.5 are visualized for 2019 and the 2030 reference scenario, showing values above 5 µg/m^3 in red and below in blue. The two scenarios for 2030 show very similar results for PM2.5, therefore the alternative scenario is not included in the figure.

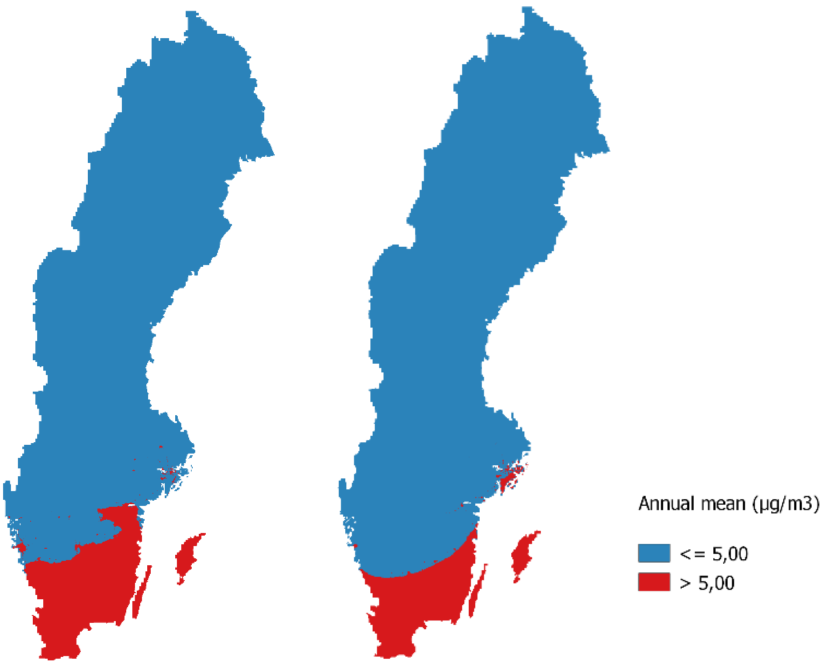

Figure 12. Annual mean concentrations for PM2.5 for 2019 (left) and the 2030 reference scenario (right). Concentrations above 5 µg/m^3 is indicated in red and below in blue.

4.1.2 Concentrations of NO_2

The annual mean concentrations of NO_2 are presented for 2019, for the 2030 reference scenario as well as the alternative scenario in Figure 13. A clear decrease in concentrations is seen from 2019 to 2030 for all of Sweden, particularly in major cities and along major roads. Swedish NO_x emissions are expected to decrease by 35% from 2019 to 2030 reference scenario (see Table 2). For example, road transport emissions are expected to decrease by 65% and "other sources", including work machines, by 40%.

A small decrease is seen for NO_2 concentrations in the alternative scenario compared to the reference scenario, mostly close to large industrial point sources. The expected emission reduction is 4% from 2030 reference scenario to 2030 alternative scenario, mostly in the sectors Public power and Industry.

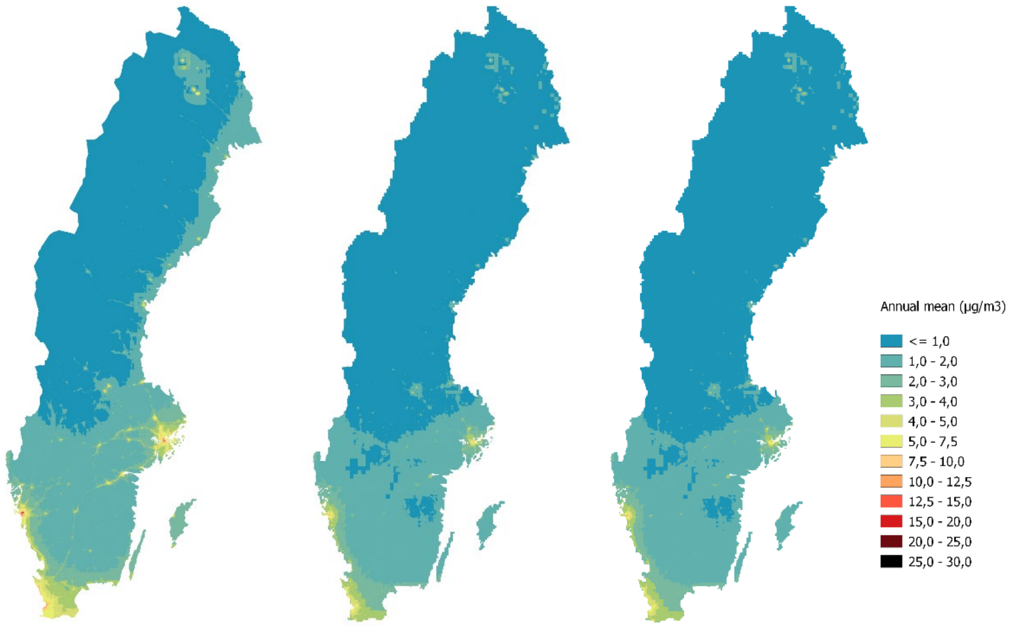

Figure 13. Annual mean concentrations of NO_2 for 2019 (left) and 2030, the reference scenario (middle) and the alternative scenario (right) on 250 m resolution.

The relation between regional and urban contribution to NO_2, as well as the total concentration levels differ depending on location in Sweden. An example for 2019 and 2030 reference scenario, seen in Figure 14, illustrates the difference between the contributions in the four cities of Malmö, Gothenburg, Stockholm and Umeå. This example can give an indication of how the expected emission reductions affect the NO_2 concentrations in different locations. All contributions are decreased in 2030 compared to 2019, and in Umeå the concentration levels are expected to decrease by 50%. As all four locations are in the city centers, the urban contributions are decreased more than the regional contributions.

The modelled concentrations are representative for the 250 m grid cell where the urban monitoring stations Malmö "Rådhuset", Gothenburg "Femman", Stockholm "Torkel Knutssongatan" and Umeå "Västra Esplanaden" are located.

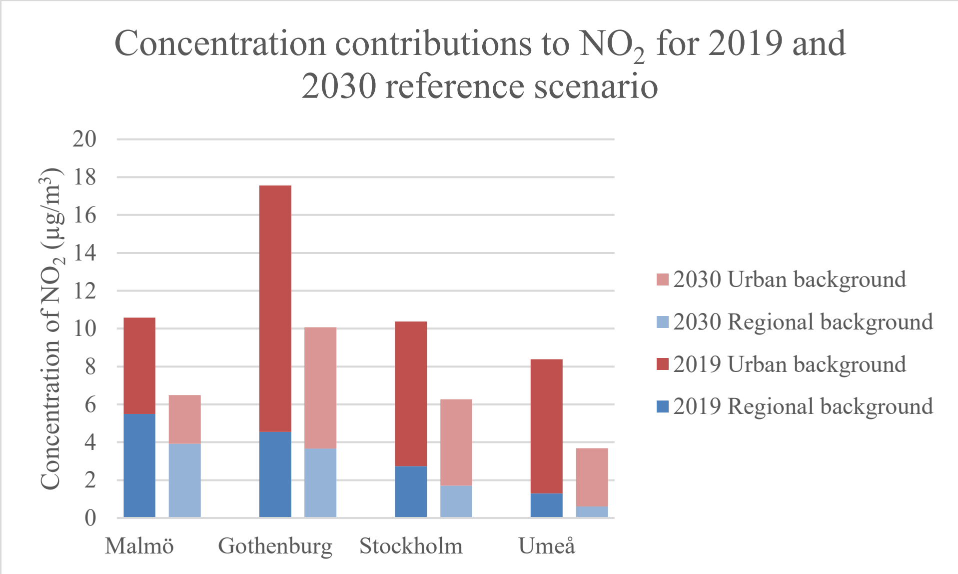

Figure 14. Regional and urban contributions to NO_2 grid concentrations for 2019 and the 2030 reference scenario at urban monitoring station locations in the four cities Malmö, Gothenburg, Stockholm and Umeå in Sweden.

Due to the non-linear behavior of NO_2 in the relationship between NO_x emissions and the resulting NO_2 levels, the urban contributions from different sources cannot be separated in a meaningful way. Instead the source contributions to NO_x ($NO+NO_2$) can indicate which emission sources are dominant in different locations. In Figure 15 the urban source contribution to NO_x concentrations are visualized in pie charts for the four cities of Malmö, Gothenburg, Stockholm and Umeå. Malmö and Gothenburg have quite similar urban contributions, Stockholm has a larger contribution from other urban sources, and in Umeå the contribution from traffic exhaust is completely dominant.

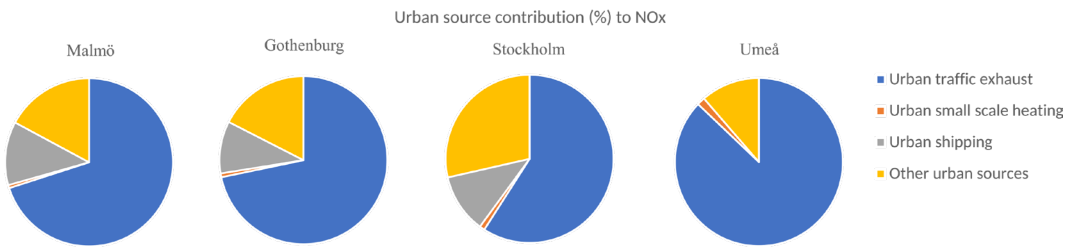

Figure 15. The urban source contribution to NO_x concentrations for 2019 are shown in pie charts for Malmö, Gothenburg, Stockholm and Umeå. Urban contributions from traffic exhaust, small-scale residential heating, shipping and other sources are presented.

4.1.3 Concentrations of PM10

The annual mean concentrations of PM10 are presented for 2019, for the 2030 reference scenario as well as the alternative scenario in Figure 16. There is a clear south/north gradient in concentration levels, with higher concentration levels in Skåne and lower concentration levels further north. PM10 levels are generally higher in medium and large cities and along the major roads.

There is a small decrease in concentrations from 2019 to 2030, however the two scenarios for 2030 are almost identical in emission totals. A very large portion of the PM10 concentrations come from a regional contribution, so a decrease in Swedish PM10 emissions, however important, give quite a small effect on Swedish total concentrations. The decrease in Swedish emissions will give a more significant effect on the highest daily mean values, which are in general more influenced by local emissions. Also note that a significant portion of PM10 emissions come from natural sources, which are not expected to decrease from 2019 to 2030.

As seen in Table 2, a reduction of Swedish PM10 emissions of 24% is expected, excluding the non-exhaust traffic contribution. The traffic emissions of PM10 are in total however expected to increase to 2030 due to higher non-exhaust emissions. Comparing the difference in emissions from 2030 reference scenario to 2030 alternative scenario conclude that they only differ by 0.1%. The very similar PM10 concentrations for the two scenario years are thus expected.

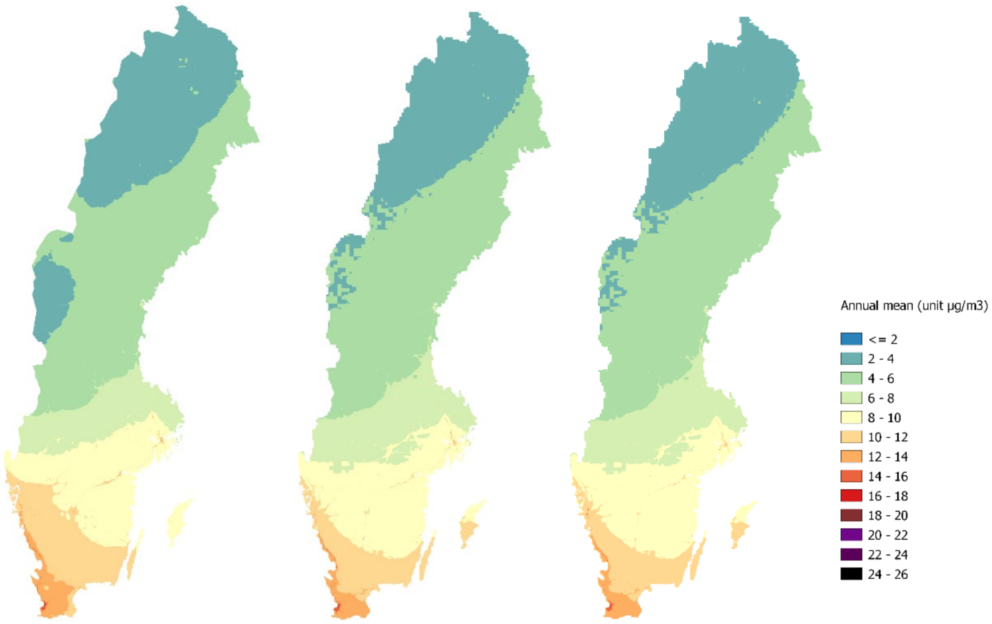

Figure 16. Annual mean concentrations of PM10 for 2019 (left) and 2030, the reference scenario (middle) and the alternative scenario (right).

In Figure 17 the regional and urban concentration contributions for the four cities of Malmö, Gothenburg, Stockholm and Umeå are presented for 2019 and 2030 reference scenario. It is clear that the regional contribution is higher in Malmö, and decreasing further north. The largest cities of Gothenburg and Stockholm have a higher urban contribution than Malmö and Umeå. There are small changes in PM10 concentrations when comparing 2019 to 2030 in these four cities. The regional contribution is slightly higher in 2030 in Malmö and Stockholm, due to international shipping. It is to be noted that the international emissions have different data sources and resolution between the two years, which might affect the results.

Figure 18 shows the urban source contributions to PM10 for the four cities. It is clear that non-exhaust traffic emissions are dominant in all cities. In Umeå, furthest north, small-scale residential heating is also a large urban contributor.

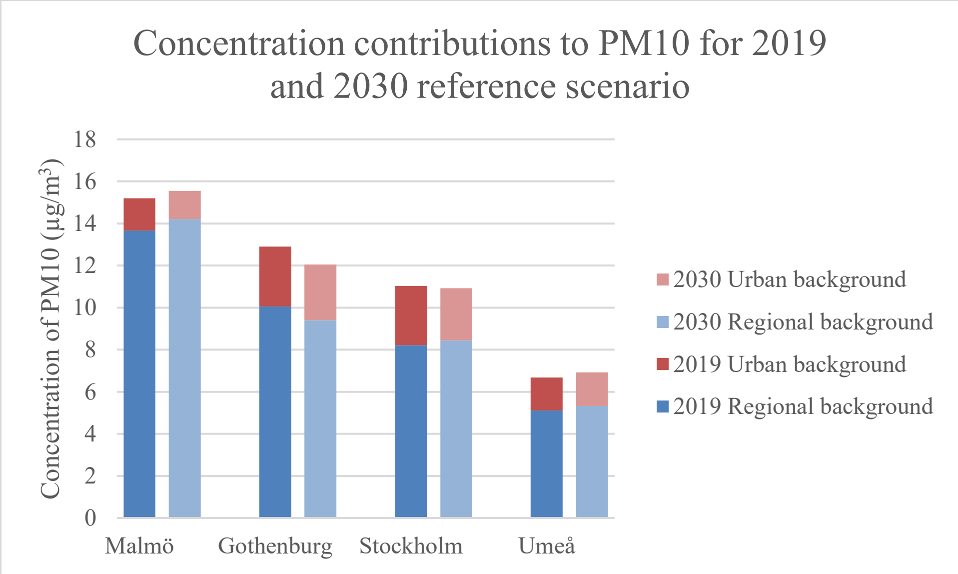

Figure 17. Regional and urban contributions to PM10 grid concentrations for 2019 and 2030 reference scenario at urban monitoring station locations in the four cities Malmö, Gothenburg, Stockholm and Umeå in Sweden.

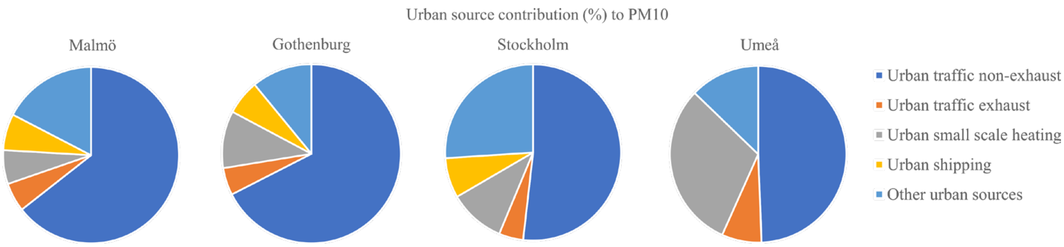

Figure 18. The urban source contribution to PM10 concentrations for 2019 are shown in pie charts for Malmö, Gothenburg, Stockholm and Umeå. Urban contributions from traffic - non-exhaust and exhaust, small-scale residential heating, shipping and other sources are presented.

4.1.4 Concentrations of PM2.5

The annual mean concentrations of PM2.5 are presented for 2019, for the 2030 reference scenario as well as the alternative scenario in Figure 19.

As for PM10, PM2.5 has a large regional background contribution, and concentration levels are higher in the south and decreasing further north. The urban contribution to PM2.5 is significant from several emission sectors, unlike for PM10 which has a majority of its urban contribution from non-exhaust traffic emissions. The major highways are thus less obvious in the concentration maps.

The concentrations of PM2.5 decrease from 2019 to 2030, but only slightly. This despite a large decrease in Swedish emissions, approximately by 24% (excluding non-exhaust traffic emissions). There are several explanations for this rather low effect on concentrations. An integral part of PM2.5 consists of natural particles, for example sea salt and biogenic secondary organic aerosols (SOA). These natural contributions are not expected to decrease from 2019 to 2030. Also, small particles travel far, and PM2.5 concentrations over Sweden are influenced by regional transport from other countries. There are also chemical aspects to consider for particles. The Swedish primary emissions of PM2.5 are expected to decrease by 24% but in regional background a larger part of the concentration consists of secondary particles formed from e.g. NO_x emissions, ammonia and SO2, and from volatile organic compounds (VOCs; largely from forests).

The largest concentration reductions for 2030 are seen in southern Sweden, where international contribution is largest. This reduction is primarily due to expected European emission reductions of PM2.5 in the European emission dataset.

The emission sectors industry and ”other sources”, including machinery, have the largest expected reduction, over 40%, compared to 2019 for PM2.5. In some locations the reduction in concentrations is clear, for example near larger industrial facilities on the north east coast and around Kiruna and Gällivare.

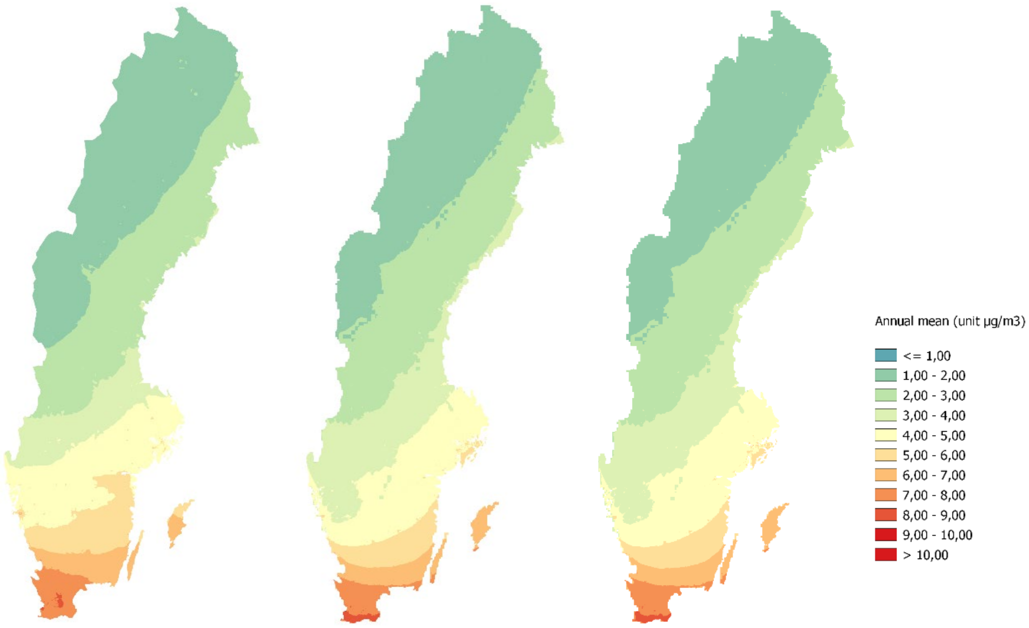

Figure 19. Annual mean concentrations of PM2.5 for 2019 (left) and 2030, the reference scenario (middle) and the alternative scenario (right).

Figure 20 illustrates the regional and urban concentration contribution to PM2.5 in 2019 and 2030 reference scenario for the four cities of Malmö, Gothenburg, Stockholm and Umeå. The pattern is very similar to the pattern of PM10, with large regional contributions, higher in the south and decreasing further north. The urban contribution is larger for Gothenburg and Stockholm than the smaller cities of Malmö and Umeå.

The regional contribution of PM2.5 is slightly higher in 2030 in Malmö and Stockholm, due to international shipping. It is to be noted that the international emissions have different data sources and resolution between the two years, which might affect the results.

The urban source contribution in Figure 21 shows that many sectors contribute to the urban concentration contribution. In Malmö and Stockholm “other urban sources” contribute most, and in Umeå the contribution from small-scale residential heating is dominant.

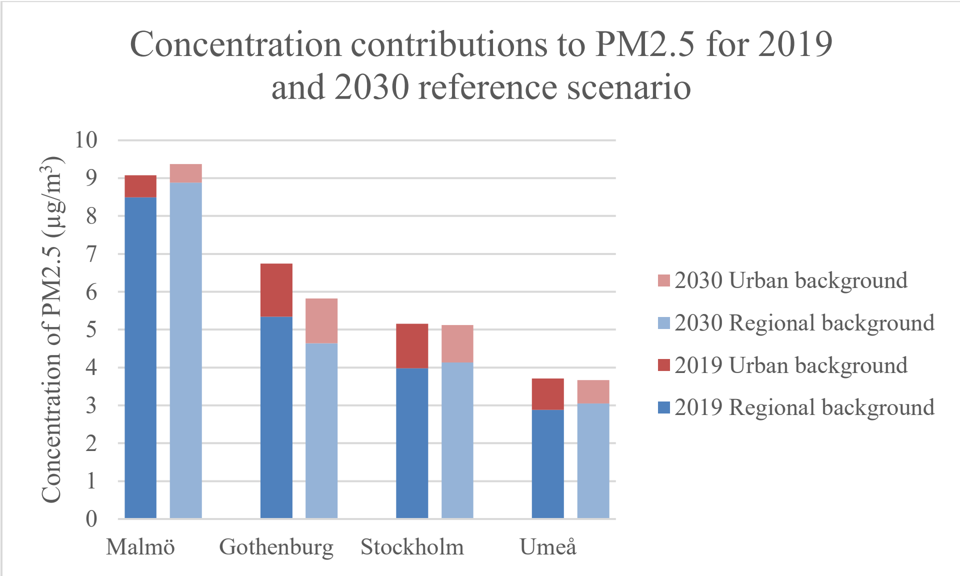

Figure 20. Regional and urban contributions to PM2.5 grid concentrations for 2019 and 2030 reference scenario at urban monitoring station locations in the four cities Malmö, Gothenburg, Stockholm and Umeå in Sweden.

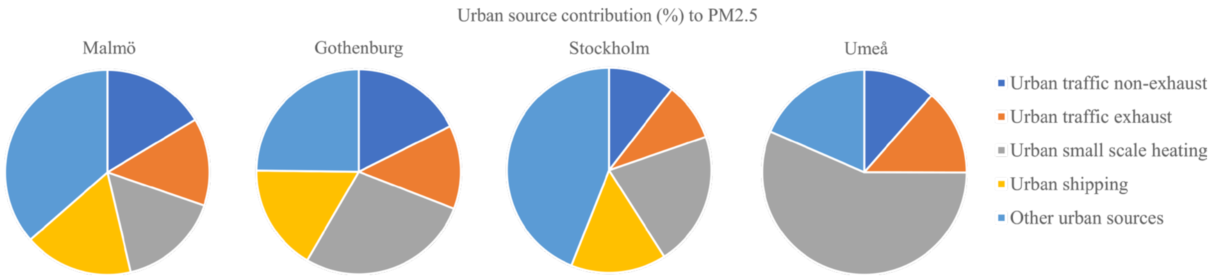

Figure 21. The urban source contribution to PM2.5 concentrations for 2019 are shown in pie charts for Malmö, Gothenburg, Stockholm and Umeå. Urban contributions from traffic - non-exhaust and exhaust, small-scale residential heating, shipping and other sources are presented.

4.2 Population exposure

In this section the population exposure results are presented for NO_2, PM10 and PM2.5, both for 2019 and the two scenarios for 2030. The same number of inhabitants in Sweden are assumed for 2030 as for 2019. This assumption is made in order to be able to analyse the effect of expected emission reductions on health outcomes.

The total population in Sweden in 2019 was 10 312 871 inhabitants. In Table 5 the number of inhabitants is presented per age span.

Table 5. Number of inhabitants in Sweden per population age span for 2019.

Population age span	Number of inhabitants
0-15	1 950 810
16-20	568 698
21-30	1 358 222
31- 50	2 636 531
51-65	1 842 658
Above 65	1 955 952
Total	10 312 871

In Table 6 exposure results are presented for NO_2, PM10 and PM2.5 for 2019, the 2030 reference scenario and the 2030 alternative scenario. The mean population weighted exposure indicate the average annual mean concentration that each person in Sweden is exposed to. A large decrease, by more than 2 µg/m^3**,** is seen for exposure to NO_2 in 2030 compared to 2019. The exposure to PM10 and PM2.5 is also decreasing in 2030, but not as drastically.

Percentage of the population exposed to levels exceeding annual air quality standards, environmental objectives and WHO guidelines is also presented in Table 6. Zero percent of the population is exposed to levels above the annual air quality standards for NO_2, PM10 and PM2.5 for 2019 and 2030. Note that model results represent urban background, not local hotspot concentrations.

For NO_2, 0.1% of the population is exposed to levels above the air quality objective in 2019, but in 2030 none of the population is exposed to exceedances. In relation to the WHO guideline 9% of the population is exposed to NO_2 levels above 10 µg/m^3 in 2019. This number decreased to 0.4% in 2030.

For PM10 1.4% of the population is exposed to levels above the environmental objective (and the WHO guideline as they are the same) in 2019. In 2030 the percentage is increased to 2.3% due to slightly higher regional concentrations in southern Sweden, and total PM10 concentrations around Malmö are very close to 15 µg/m^3.

Regarding PM2.5 there is no exposure to levels above the environmental objective of 10 µg/m^3, however 47% of the population is exposed to levels above 5 µg/m^3 in 2019 and 35% in 2030.

Table 6. Exposure results presented for NO_2, PM10 and PM2.5 for 2019 and 2030 reference scenario and alternative scenario. Percentage of population exposed to concentration levels exceeding air quality standards, air quality objectives and WHO guideline is presented.

	Year/scenario	NO_2	PM10	PM2.5
Mean population weighted exposure (annual mean, µg/m^3)	2019	5.08	9.95	5.21
	2030 reference scenario	3.10	9.72	5.01
	2030 alternative scenario	3.03	9.72	5.01
Percentage of population exposed to levels exceeding the Air quality standard (annual mean, µg/m^3)	2019	0% > 40	0% > 40	0% > 25
	2030 reference scenario	0% > 40	0% > 40	0% > 25
	2030 alternative scenario	0% > 40	0% > 40	0% > 25
Percentage of population exposed to levels exceeding the Air quality objective (annual mean, µg/m^3)	2019	0.1% > 20	1.4% > 15	0% > 10
	2030 reference scenario	0% > 20	2.3% >15	0% > 10
	2030 alternative scenario	0% > 20	2.3% >15	0% > 10
Percentage of population exposed to levels exceeding the WHO guideline (annual mean, µg/m^3)	2019	9.2% > 10	1.4% > 15	47% > 5
	2030 reference scenario	0.4% > 10	2.3% >15	35% > 5
	2030 alternative scenario	0.4% > 10	2.3% >15	35% > 5

In Table 7 exposure results are presented per age group for NO_2, PM10 and PM2.5 in 2019, and results for 2030 are seen in Table 8. A general conclusion is that exposure is higher in the age span of 21-50 years. An explanation is that these age groups more often live in urban areas, where there are more emissions and higher concentrations of pollution.

Table 7. Exposure results presented per age group for NO_2, PM10 and PM2.5 for 2019.

Mean population weighted exposure (µg/m^3)	NO_2	PM10	PM2.5
Total population	5.08	9.95	5.21
Age 0-15 years	4.92	9.96	5.21
Age 16-20 years	4.85	9.90	5.19
Age 21-30 years	5.79	10.18	5.30
Age 31-50 years	5.35	10.07	5.25
Age 51-65 years	4.88	9.84	5.16
Age 66+ years	4.66	9.73	5.13

Table 8. Exposure results presented per age group for NO_2, PM10 and PM2.5 for 2030. Note that both scenarios give the same exposure results for particulate matter.

Pollutant	NO_2	NO_2	PM10	PM2.5
Mean population weighted exposure (µg/m^3)	**2030 reference scenario**	**2030 alternative scenario**	**2030 reference scenario and alternative scenario**	**2030 reference scenario and alternative scenario**
Total population	3.10	3.03	9.72	5.01
Age 0-15 years	3.02	3.00	9.74	5.02
Age 16-20 years	2.97	2.91	9.67	4.99
Age 21-30 years	3.46	3.38	9.93	5.08
Age 31-50 years	3.24	3.17	9.84	5.05
Age 51-65 years	3.00	2.94	9.62	4.96
Age 66+ years	2.88	2.82	9.52	4.93

4.2.1 Exposure to NO_2

In Table 9 the exposure contribution from urban sources and regional background is shown for 2019, 2030 reference scenario and the 2030 alternative scenario. A slight majority of the exposure contribution come from regional background. In the 2030 scenarios the urban contribution decreased more than the regional contribution, compared to 2019.

Table 9. Exposure results for NO_2 presented as a contribution from urban sources and regional background for 2019, 2030 reference scenario and 2030 alternative scenario.

Year/scenario	2019	2030 reference scenario	2030 alternative scenario
Mean population weighted exposure (µg/m^3)	5.08	3.10	3.03
Exposure contribution from urban sources (µg/m^3)	2.52	1.25	1.21
Exposure contribution from regional background (µg/m^3)	2.56	1.85	1.82

In Figure 22 the number of people exposed to different concentration intervals of NO_2 is shown and also presented per age group. About 6 million people are exposed to NO_2 annual concentrations of maximum 5 µg/m^3, roughly another 3 million are exposed to levels between 5 and 10 µg/m^3 and less than one million people are exposed to levels above 10 µg/m^3 in 2019.

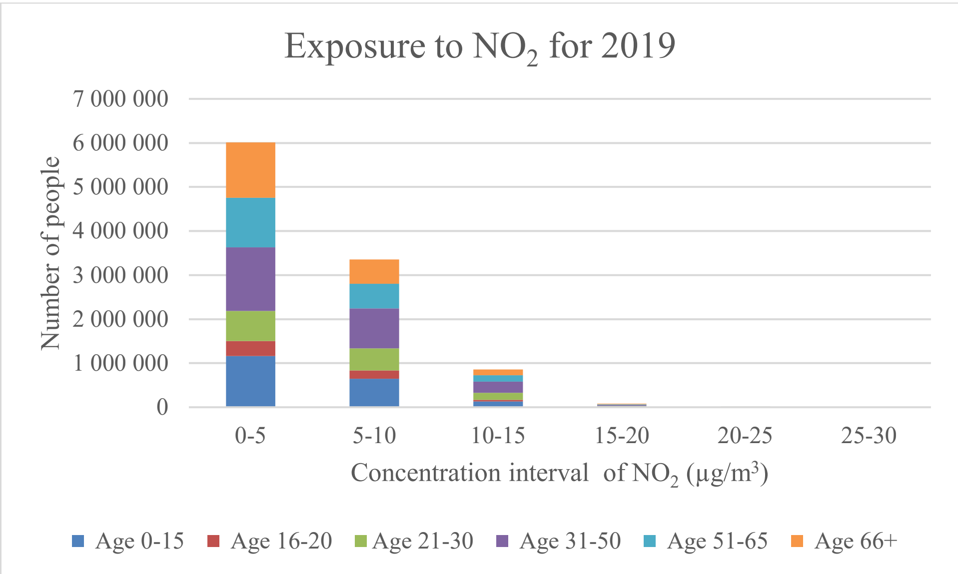

Figure 22. Number of people exposed to NO_2 in concentration intervals, presented per age span interval for 2019.

In Figure 23 the exposure to NO_2 for different concentration intervals is seen for 2019 and the two scenarios for 2030. A clear shift towards lower exposure is seen for the 2030 scenarios compared to 2019, where more people are exposed to low concentration levels (up to 4 µg/m^3) in 2030 compared to 2019.

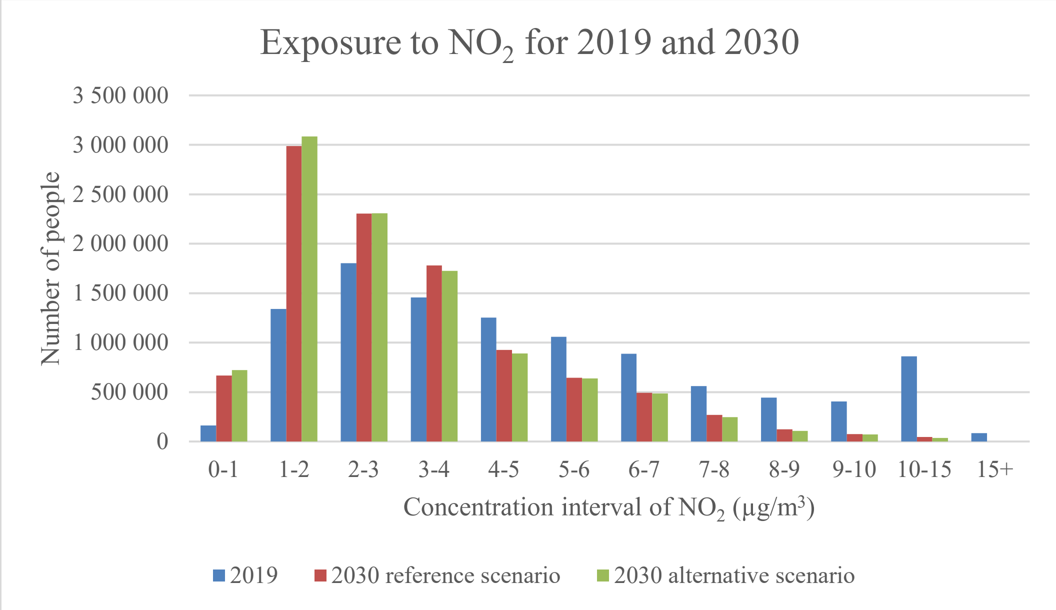

Figure 23. Exposure to NO_2 presented for 2019, the 2030 reference scenario and the alternative scenario in concentration intervals. Note that above 10 $\mu g/m^3$ the bins are larger.

In Figure 24 the source contribution to mean population weighted exposure is seen for NO_x for 2019, 2030 reference scenario and 2030 alternative scenario. The urban NO_x contributions decreased from 2019 to 2030 relative to the regional background contribution. Especially exposure to urban traffic exhaust has reduced by 2030.

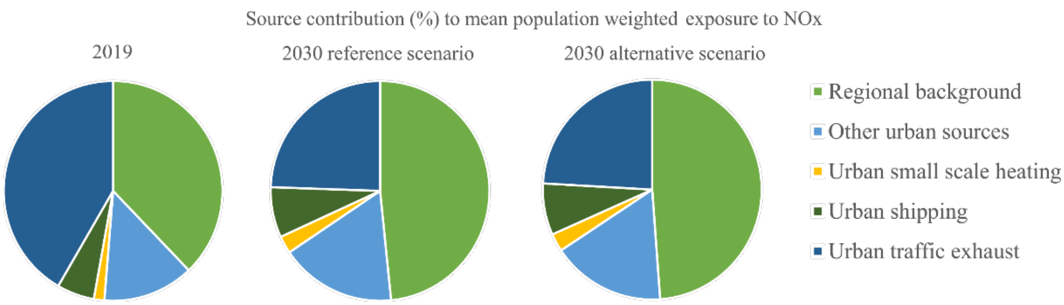

Figure 24. Source contribution to mean population weighted exposure to NO_x for 2019, the 2030 reference and alternative scenario.

4.2.2 Exposure to PM10 and PM2.5

In Table 10 and Table 11 exposure results are presented for 2019 and 2030 for different source contributions to PM10 and PM2.5. Note that the two scenarios for 2030 are so similar that the exposure results are the same. The regional background exposure is dominant, both for 2019 and 2030 for particulate matter. The urban contributions to exposure are similar for PM10 and PM2.5 for small-scale residential heating, shipping and exhaust emissions from traffic. For non-exhaust traffic emissions PM10 has significantly larger exposure contribution than PM2.5, by approximately a factor of 10. Also exposure from other urban sources is larger for PM10 than PM2.5.

The calculated exposure reduction from 2019 to 2030 is about 0.2 µg/m^3 for both PM10 and PM2.5. About half of the reduction is from regional background and the other half from reductions of small-scale residential heating, exhaust emissions from traffic and other urban sources.

Table 10. Exposure results presented for different source contributions for PM10 and PM2.5 for 2019.

Pollutant	PM10	PM2.5
Mean population weighted exposure (µg/m^3)	9.95	5.21
Exposure contribution from urban small-scale residential heating (µg/m^3)	0.18	0.18
Exposure contribution from urban shipping (µg/m^3)	0.03	0.03
Exposure contribution from urban road traffic (exhaust) (µg/m^3)	0.04	0.03
Exposure contribution from urban road traffic (non-exhaust) (µg/m^3)	0.58	0.05
Exposure contribution from other urban sources (µg/m^3)	0.15	0.11
Exposure contribution from regional background (µg/m^3)	8.97	4.80

Table 11. Exposure results presented for different source contributions for PM10 and PM2.5 for 2030. The two scenarios have the same exposure results for PM.

Pollutant	PM10	PM2.5
Mean population weighted exposure (µg/m^3)	9.72	5.01
Exposure contribution from urban small-scale residential heating (µg/m^3)	0.13	0.13
Exposure contribution from urban shipping (µg/m^3)	0.04	0.04
Exposure contribution from urban road traffic (exhaust) (µg/m^3)	0.02	0.01
Exposure contribution from urban road traffic (non-exhaust) (µg/m^3)	0.56	0.06
Exposure contribution from other urban sources (µg/m^3)	0.12	0.09
Exposure contribution from regional background (µg/m^3)	8.87	4.69

In Figure 25 the number of people exposed to different concentration intervals of PM10 is shown and presented per age group for 2019. Most of the population is exposed to levels between 5 and 15 µg/m³.

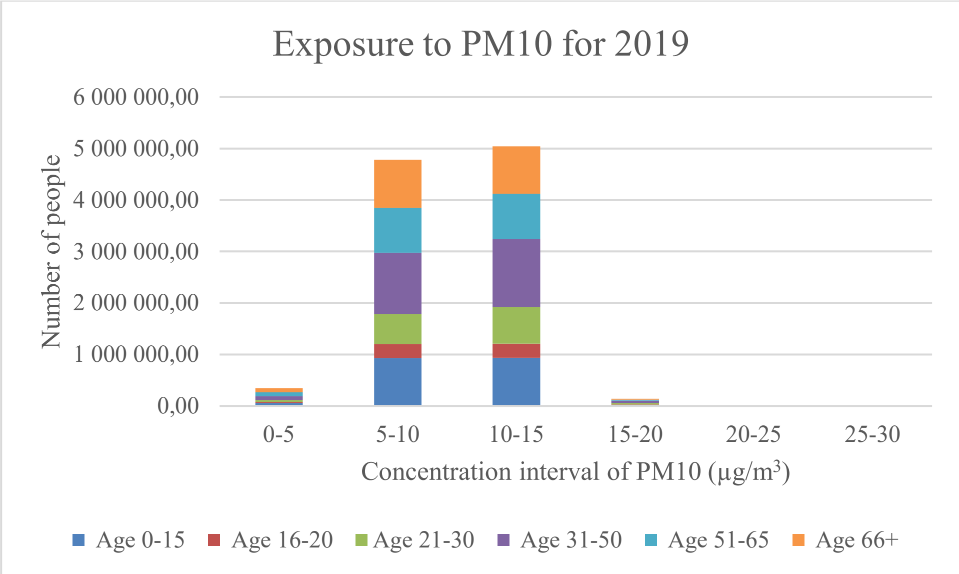

Figure 25. Number of people exposed to PM10 in concentration intervals, presented per age span interval for 2019.

Figure 26 presents the exposure contributions to PM10. The bar chart to the left illustrates the regional background and urban contributions to exposure, and the pie chart to the right presents the urban contributions from different urban sources. It is clear that the regional contribution is dominant, and in regards to urban contributions, the non-exhaust traffic emissions contribute to the majority of the urban exposure.

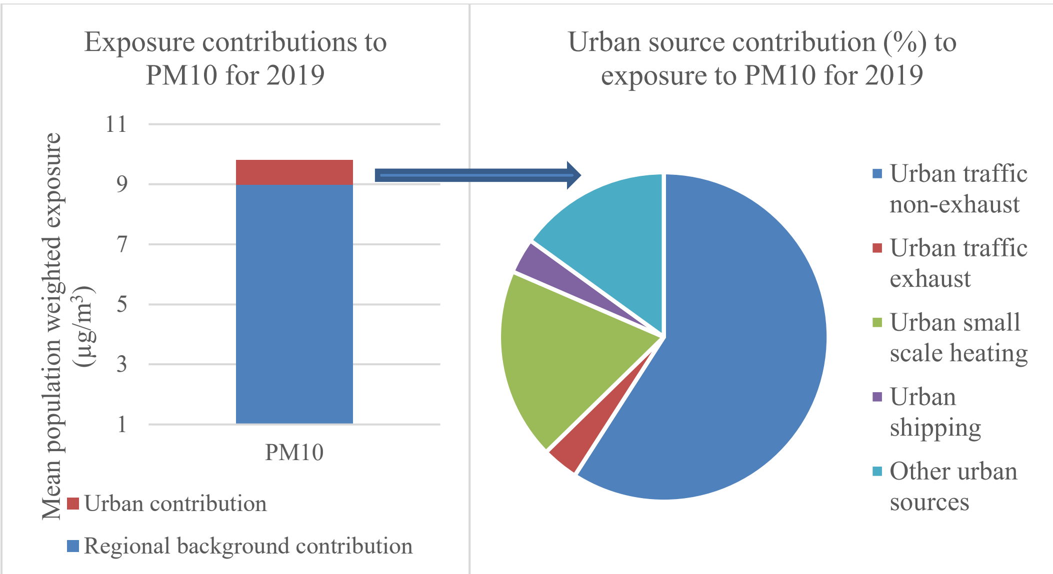

Figure 26. Exposure contributions to PM10, divided into a regional and an urban contribution (left) and the urban exposure contribution further divided into

contributions from traffic - non-exhaust and exhaust, small-scale residential heating, shipping and other sources (right).

Figure 27 shows the number of people exposed to different concentration intervals of PM10 for the 2030 reference scenario. Figure 28 shows a comparison between the exposure to PM10 for 2019 and the 2030 reference scenario. There is a reduction in exposure from 2019 to 2030, however there are slightly more people exposed to PM10 concentrations above 15 µg/m^3 in 2030. This is because of slightly higher concentrations in Malmö due to small differences in the regional background between 2019 and 2030, where 2030 showed higher PM10 emissions from international shipping and the total PM10 concentrations are very close to 15 µg/m^3.

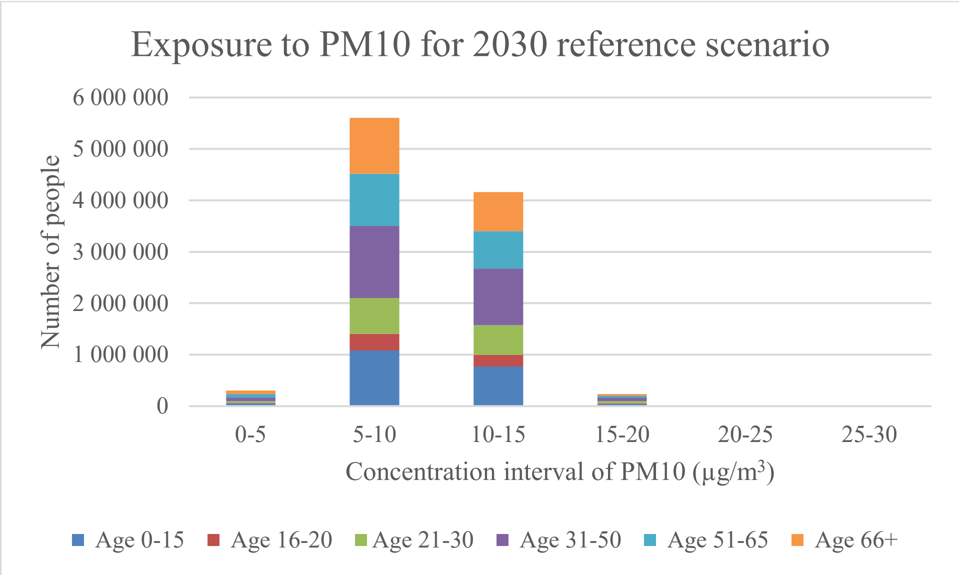

Figure 27. Number of people exposed to PM10 in concentration intervals, presented per age span interval for the 2030 reference scenario.

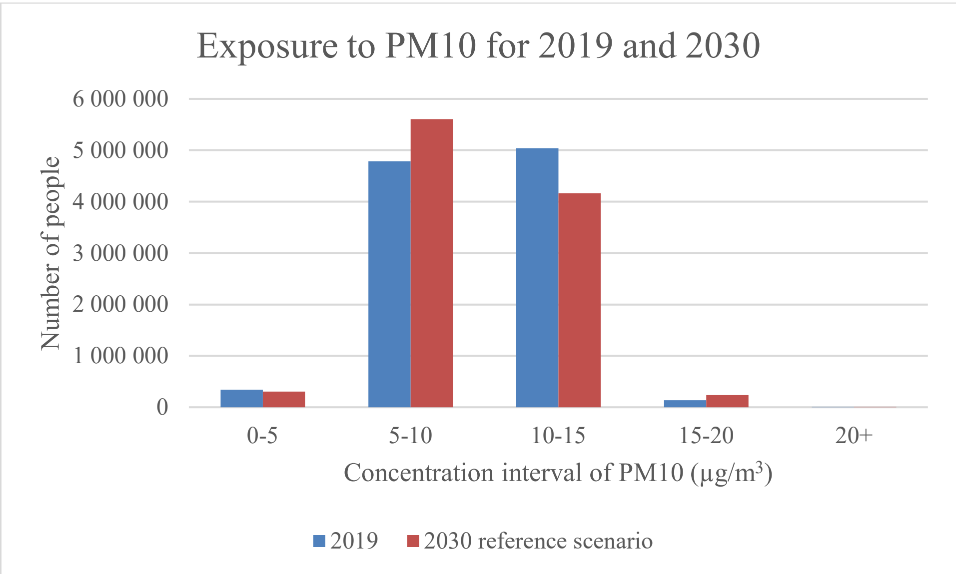

Figure 28. Exposure to PM10 for 2019 and the 2030 reference scenario.

Figure 29 shows the number of people exposed to different concentration intervals of PM2.5, per age group for 2019. Slightly more than 6 million people are exposed to PM2.5 concentrations in the interval 4-6 μg/m^3.

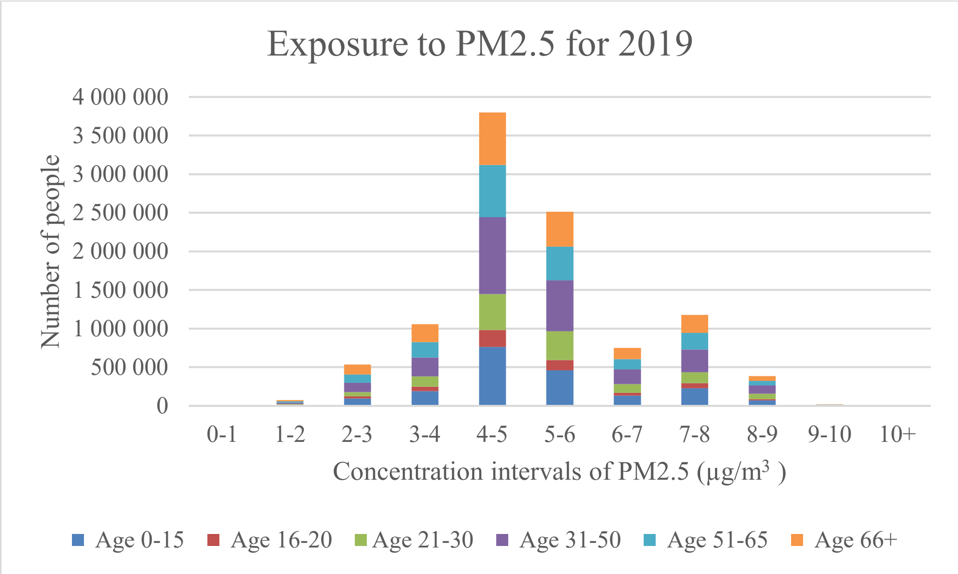

Figure 29. Number of people exposed to PM2.5 in concentration intervals, presented per age span interval for 2019.

Figure 30 presents the exposure contributions to PM2.5. The bar chart to the left illustrates the regional background and urban contributions to exposure, and the pie chart to the right presents the urban contributions from different urban sources. The regional contribution is very dominant, and in regards to urban contributions, several sources contribute significantly. Small-scale residential heating is the largest sector contributor to the urban exposure, followed by other urban sources.

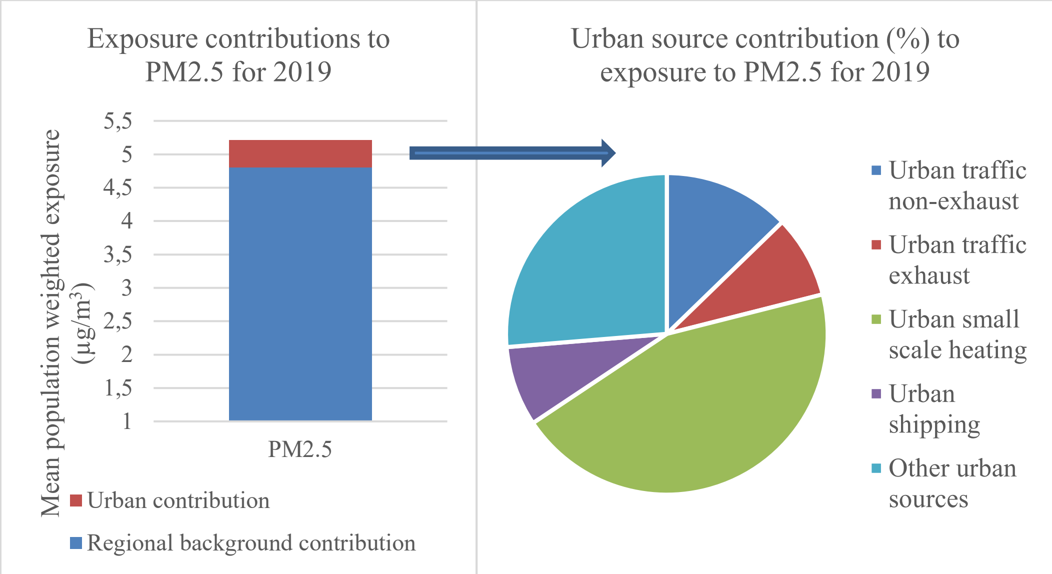

Figure 30. Exposure contributions to PM2.5, divided into a regional and an urban contribution (left) and the urban exposure contribution further divided into contributions from traffic - non-exhaust and exhaust, small-scale residential heating, shipping and other sources (right).

Figure 31 shows the number of people exposed to different concentration intervals of PM2.5 for the 2030 reference scenario. Figure 32 shows a comparison between the exposure to PM10 for 2019 and the 2030 reference scenario. There is a reduction in exposure from 2019 to 2030. Table 12 presents the number of people exposed to PM2.5 concentrations above 5 µg/m^3 (the WHO guideline) for 2019, 2030 reference and 2030 alternative scenarios. About 1.2 million less people are exposed to levels above 5 µg/m^3 in 2030. Approximately 40 000 less people are exposed to levels over the WHO guideline in the 2030 alternative scenario compared to the 2030 reference scenario. However 35% of the Swedish population is still exposed to levels above the WHO guideline in 2030.

In Table 12 the number of people exposed to PM2.5 levels above 5 µg/m^3 is listed per age group for 2019 and 2030 reference scenario, together with the average exposure for those exposed to levels above 5 µg/m^3. Fewer people are exposed to levels above 5 µg/m^3 in 2030, but the average exposure for those who are exposed to levels above 5 µg/m^3 is slightly higher in 2030, indicating a sharper gradient in concentration decrease over Sweden.

In Table 13 the number of people exposed to PM2.5 levels above 5 µg/m^3 in 2019 and the 2030 reference scenario is presented. The average exposure to PM2.5 is presented for those who are exposed to levels above 5 µg/m^3.

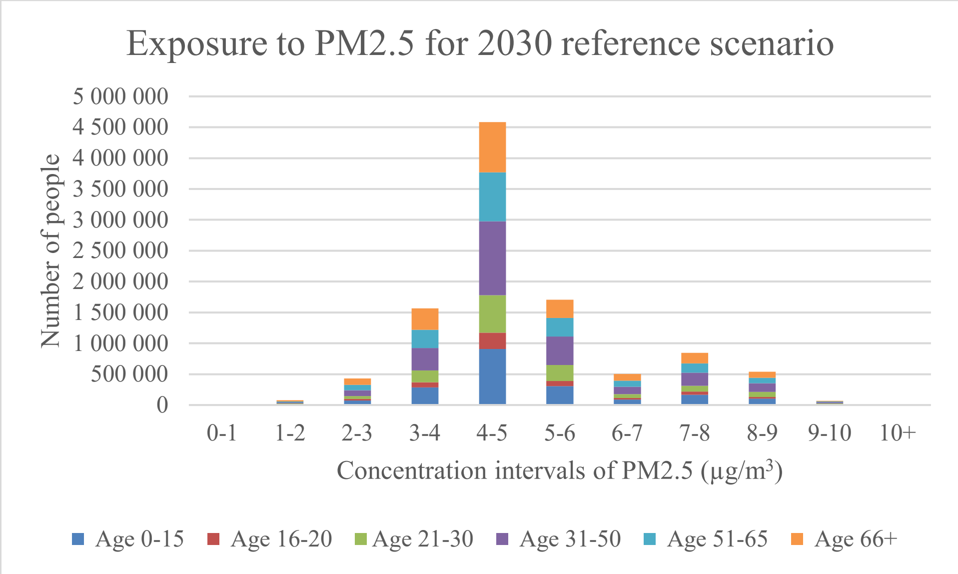

Figure 31. Number of people exposed to PM2.5 in concentration intervals, presented per age span interval for the 2030 reference scenario.

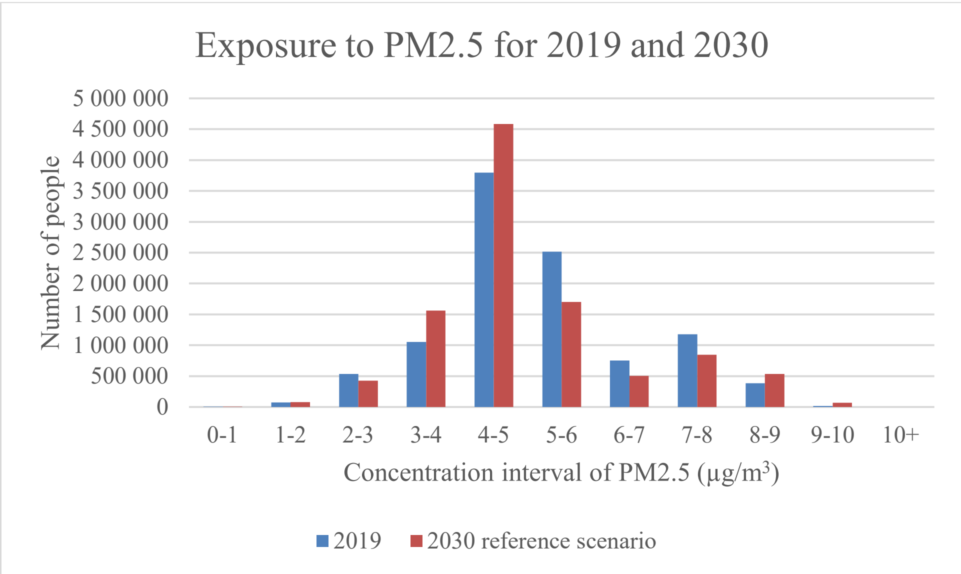

Figure 32. Exposure to PM2.5 for 2019 and the 2030 reference scenario.

Table 12. Number of people exposed to PM2.5 levels above 5 µg/m^3 for 2019, 2030 reference scenario and 2030 alternative scenario.

Year/scenario	**2019**	**2030 reference scenario**	**2030 alternative scenario**
Number of people exposed to PM2.5 levels > 5 µg/m^3	4 848 125	3 658 046	3 619 908

Table 13. Number of people exposed to PM2.5 levels above 5 µg/m³ in 2019 and the 2030 reference scenario. The average exposure to PM2.5 is presented for those who are exposed to levels above 5 µg/m³.

Year/scenario	2019		2030 reference scenario	
	Number of people exposed > 5 µg/m³	**PM2.5 exposure where > 5 µg/m³**	**Number of people exposed > 5 µg/m³**	**PM2.5 exposure where > 5 µg/m³**
Age 0-15 years	890 686	6.31	671 825	6.54
Age 16-20 years	259 661	6.29	192 726	6.54
Age 21-30 years	696 944	6.27	510 050	6.48
Age 31-50 years	125 7616	6.29	960 629	6.48
Age 51-65 years	845 392	6.29	645 576	6.49
Age 66+ years	897 826	6.31	677 243	6.53

4.3 Estimated health impacts

4.3.1 Mortality

The modelled population exposure for 2019 was used to calculate preterm mortality in persons older than 30 years of age, assuming different exposure-response functions for regional background PM2.5 and PM2.5 from urban sources, and an impact on mortality of NO_2 itself only for the urban contribution of NO_2 (Table 14).

Table 14. Long-term exposure and premature deaths per year (with lower and upper 95% confidence interval limits) in persons older than 30 years of age.

Type of exposure	Estimate	95% LCL	95% UCL
Regional background PM2.5	3 296	*2 408*	*3 566*
Urban small-scale residential heating PM2.5	433	*318*	*457*
Urban shipping PM2.5	80	*59*	*85*
Urban traffic exhaust PM2.5	79	*58*	*84*
Urban traffic non-exhaust PM2.5	122	*89*	*128*
Other urban sources PM2.5	254	*187*	*268*
Urban sources NO_2	428	*213*	*841*
Total (urban sources)	**4 692 (1 396)**		

When adding the yearly number of preterm deaths attributed to the regional background PM2.5 levels and to the PM2.5 exposure from urban sources, the total number becomes 4 264 deaths. When the yearly number of preterm deaths attributed to PM2.5 and to NO_2 from urban sources are added, the total number becomes 1 396 deaths. The premature deaths attributed to the regional background levels, plus the deaths due to the urban source contribution, totally become 4 692 premature deaths per year.

If the effect of PM2.5 on total mortality only exist above an annual mean of 5 µg/m^3 and a relative risk of 1.08 per 10 µg/m^3 (95% CI 1.06 – 1.09) is assumed, the estimate total number of premature deaths becomes 417 (95% CI 304 – 451). If the effect of PM2.5 only exist above an annual mean of 5 µg/m^3 but the relative risk from the pooled cohorts in the European ELAPSE Study of 1.28 for 10 µg/m^3 (95% CI 1.22 – 1.33) is assumed (Strak et al, 2021), the estimate number of premature deaths becomes 1 443 (95% CI 1054 – 1523). When the cutoff at 5 µg/m^3 is kept, but relative risk in ELAPSE estimated for exposure levels <12 µg/m^3 of 1.68 (95% CI 1.30 – 2.73) for 10 µg/m^3 is assumed, the estimated number of deaths per year associated with exposure above 5 µg/m^3 increases to 3 542 (95% CI 1 384 – 4 204).

4.3.2 Morbidity

The impacts of PM2.5 on morbidity are calculated as existing only above an annual mean of 5 µg/m^3 without separation of the particle sources. Table 15 shows that the attributed numbers of new cases of Diabetes and Cardiovascular diseases (Stroke and Myocardial infarction) are much higher than the number of lung cancer and COPD cases.

Table 15. Long-term exposure to PM2.5 (total) above 5 µg/m3 (WHO air quality guideline) and estimated number of health outcomes per year (with lower and upper 95% confidence interval limits).

Health outcome	**Estimate**	**95% LCL**	**95% UCL**
Myocardial infarction >30 yrs	115	*10*	*216*
Stroke >30 yrs	433	*78*	*653*
Lung cancer > 30 yrs	46	*16*	*75*
Dementia >50 yrs	218	*78*	*324*
Diabetes >15 yrs	512	*196*	*745*
COPD > 50 yrs	71	*44*	*87*
Childhood astma < 20 yrs	193	*56*	*281*
Preterm birth	104	*34*	*152*

If the relative risk functions are assumed to be correct for all levels of PM2.5 and no cut off is used, the estimated yearly numbers become four times higher.

4.3.3 2030 scenarios

Actual demographic data and baseline frequencies for the health outcomes are lacking for the 2030 scenarios. If only the exposure levels would change according to the model results, the total PM2.5 exposure would be 4% lower for the total population older than 30 years of age. However, because the impact on mortality is calculated separately for the regional background and the urban sources, it is relevant to note that the first population exposure would be about 2% lower and the latter 22% lower, which indicates how much the attributed number of preterm deaths would change if everything else stays the same. As the two scenarios for 2030 are so similar for PM exposure, these conclusions are valid for both scenarios.

If instead the assumption is that there are impacts on health outcomes only when the annual mean of PM2.5 is above 5 µg/m^3, the total population exposure above 5 µg/m^3 among persons older than 30 years of age would be 12% lower in 2030 compared with the 2030 scenarios. The change is very similar for other age groups.

We assume an impact on mortality only for NO_2 from urban sources, and this population exposure would 2030 become approximately only half of the 2019 exposure.

4.4 Model validation

A model validation was carried out where model results were compared to urban background measurements. Model results were validated before an urban bias correction was applied, in order to ensure sufficient model quality also where there are no urban background measurements available.

The software DELTA tool[24], developed in the framework of FAIRMODE[25], is to support European air quality modellers in the diagnostics and assessment of air quality modelling performances under the EU 2008 Ambient Air Quality Directive (European Commission, 2022).

DELTA tool compares modelled and measured timeseries of pollutant concentrations in given locations. A minimum data availability (currently 75%) is required for statistics to be produced at a given measurement station. The software calculates a number of statistical indicators and a Model Quality Objective (MQO)[26], defined as the minimum level of quality to be achieved by a model for policy use. The MQO is constructed on the basis of the observation uncertainty.

How well model results compare to measurements at a station, according to the MQO, can be visualized in a Target diagram. If the station is plotted inside the green circle ($T<1$) the MQO is fulfilled. The Target diagram also provides information about whether the model error is dominated by bias (either negative or positive), by correlation or standard deviation. MQO must be fulfilled for at least 90% of the available stations.

In Figure 33 the Target diagram from the DELTA tool software shows the comparison of model results to urban background measurements of NO_2. There were 13 stations available with hourly data, of which 12 had a minimum data availability of 75%. The Modelling Quality Objective (MQO) is passed for 11 out of 12 stations (the comparison with the measurement site in Landskrona fails due to a very high standard deviation). The quality objective is thus met for more than 90% of the stations and the modelling system is of sufficient quality according to the validation method recommended by FAIRMODE.

In Figure 34 all PM10 stations in the Target diagram pass the MQO. There are notably only 5 stations available on an hourly resolution in urban background. The diagram shows that the model errors are dominated by low correlation, a common problem when modelling PM10.

Figure 35 shows the Target diagram for all PM2.5 stations. There are only five stations on an hourly resolution of which four have data availability over 75%. These four stations pass the MQO. Also for PM2.5 the model error is dominated by correlation issues.

To conclude, the modelling system passes the validations for NO_2, PM10 and PM2.5 according to the MQO defined in FAIRMODE.

[24] DELTA tool: https://aqm.jrc.ec.europa.eu/

[25] FAIRMODE (Forum for Air Quality Modelling in Europe): https://fairmode.jrc.ec.europa.eu/

[26] FAIRMODE guidance document on modelling quality objectives and benchmarking (version 3.3): https://data.europa.eu/doi/10.2760/41988

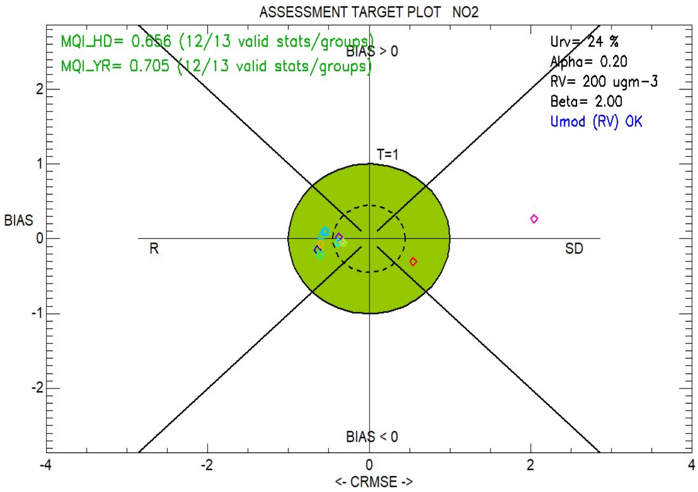

Figure 33. Target diagram from the DELTA tool software visualizing the comparison between the model results and hourly urban background measurements of NO_2. All but one station (marked with different coloured symbols) pass the MQO.

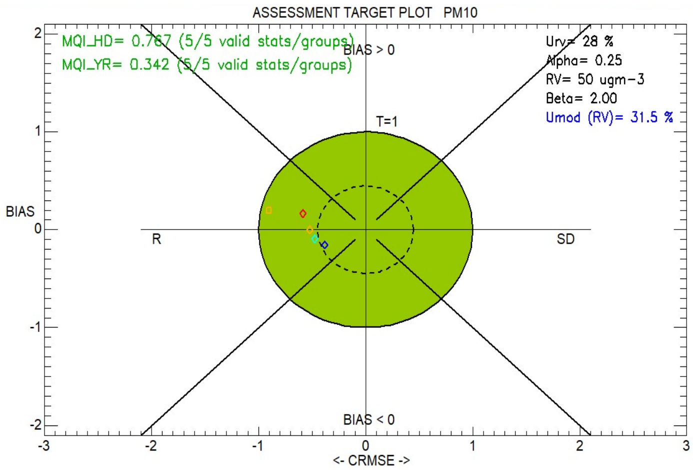

Figure 34. Target diagram from the DELTA tool software visualizing the comparison between model results and hourly urban background measurements of PM10. All stations (marked with different coloured symbols) pass the MQO.

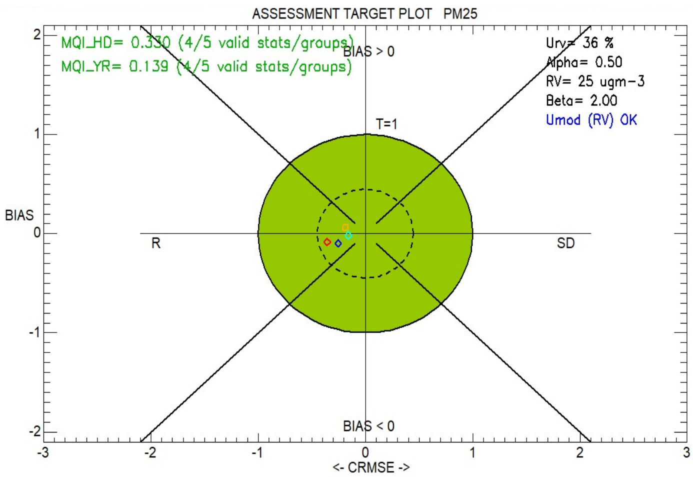

Figure 35. Target diagram from the DELTA tool software visualizing the comparison between model results and hourly urban background measurements of PM2.5. All stations (marked with different coloured symbols) pass the MQO.

5 Conclusions

5.1 Concentration levels of NO_2, PM10 and PM2.5

Concentrations of NO_2, PM10 and PM2.5 have been calculated for the whole of Sweden for the year 2019 as well as two scenarios for 2030. Calculations have been performed using a new methodology, allowing almost seam-less combination of modelling at regional and urban scale without double-counting emissions. The concentrations have been calculated at 250x250 m^2 resolution, producing a uniquely complete and detailed dataset at national scale. The methodology used can well reproduce the measured pollution levels at most urban background stations in the modelling domain. The spatial resolution of 250 m captures concentration gradients that are of importance for exposure calculations. The same modelling concept could however be applied to calculate concentrations at higher resolution. An important strength of using dispersion modelling to calculate concentrations is the direct relation with emission inventories, allowing for source attribution and scenario evaluation that is consistent with emission inventories and projections.

For NO_2, the urban sources are dominating. This is expected, considering the relatively short lifetime of NO_2 in the atmosphere. There is also a decrease in the regional contribution from the south to the north of the country. The urban source apportionment (for NO_x) is similar between the three of the four cities studied in detail (Stockholm, Gothenburg, Malmö and Umeå), where traffic is the dominating sector, while shipping and ”other” are smaller, but still important. In Umeå, the urban contribution from the shipping sector is very small.

Comparing the results for 2019 and the 2030 scenarios, mainly the urban contribution decrease, which is expected since NO_2 is dominated by contributions from local sources. Also, since the main contributing sector for NO_2 is the traffic sector, there is a large decrease in the NO_2 levels between 2019 and the 2030 scenarios. The decrease is largest in urban areas.

For PM10 the spatial pattern is rather different from NO_2. The urban contribution is much smaller and PM10 overall is more “regional” in character. The regional background decrease from the southeast to the northwest, though the Stockholm area has higher concentrations than the surrounding region. For all four cities studied in detail, non-exhaust traffic is the largest urban contributor to PM10. In Umeå, the relative contribution from small-scale residential heating is larger than for the other three cities.

Between 2019 and the two 2030 scenarios, there is only a minor decrease in the PM10 levels. Between the 2030 scenarios there is almost no difference.

For PM2.5, the spatial pattern is similar to that for PM10, though the levels are lower. Also, the regional part of the total concentrations is even higher than that for PM10. Stockholm and Malmö have similar sector contributions, where traffic is the largest contributor to the urban concentrations, while for Gothenburg small-scale residential heating is slightly larger than traffic. For Umeå, small-scale residential heating is dominating the urban concentrations, while the shipping contribution is negligible.

There are many sources of uncertainties involved in the calculated exposure. The emission inventories are probably the most important. For some sources, e.g. small-scale residential heating, also the dispersion is uncertain, given that emissions occur within residential areas and the initial dispersion is difficult to describe.

By combining dispersion modelling with available measurements, maximal use of the available information can be achieved. In this project a relatively simple bias-correction is performed using measurement data at both regional scale and urban scale. The correction is most important for PM at regional scale, where some diffuse natural sources are not included in the emission inventory. However, since this correction is carried out using the total concentrations, it does not reduce uncertainties in the relative contribution from different sources. This means that presented total concentrations are more certain than the relative contributions of different urban sources.

An uncertain assumption regarding non-exhaust emissions from traffic relates to the size-distribution of PM generated by the different wear processes. The concentrations of non-exhaust PM2.5 in this study is based on a different ratio between the fine and coarse mass in traffic non-exhaust PM10 than in other studies (Segersson et al, 2017; Söderkvist et al, 2019; Segersson et al, 2021). In this study, the default configuration of the NORTRIP model has been used, suggesting around 8% of PM10 is smaller than 2.5 micrometres in diameter (i.e. PM2.5). In previous studies a higher estimate, around 20-30%, has been used.

Despite increasing traffic volumes, the exposure due to non-exhaust PM from road-traffic shows almost no change until 2030. A possible explanation is that the change due to increased traffic volumes is largely cancelled out by the reduction in use of studded tyres in southern Sweden. There are several sources of uncertainty related to this 2030 projection, one important example being changed road wear due to heavier electric vehicles.

If 20% of traffic non-exhaust PM10 is assumed to be in the fine fraction, and the impact on mortality is calculated with the higher risk estimate for the urban contribution, the impact would be estimated higher than if the calculation is based on PM10 and a typical risk estimate of 4% per 10 µg/m^3, or the short-term effect only (Meister et al, 2012), but there would be no risk of double counting. However, in this study the impact on mortality from traffic non-exhaust PM10 is likely underestimated due to the focus on PM2.5, assuming a low proportion in non-exhaust PM10.

5.2 Population exposure

The annual average population weighted exposure is 5.08 µg/m^3 for NO_2, 9.95 µg/m^3 for PM10 and 5.21 µg/m^3 for PM2.5 in 2019. A large decrease, by approximately 2 µg/m^3**,** is seen for exposure to NO_2 in 2030 compared to 2019 (slightly more in the alternative scenario). The exposure to PM10 and PM2.5 is also decreasing in 2030, but not as drastically, by about 0.2 µg/m^3.

A general conclusion is that exposure is higher in the age span of 21-50 years. An explanation is that these age groups more often live in urban areas, where there are more emissions and higher concentrations of pollution.

Zero percent of the population is exposed to levels above the annual air quality standards for NO_2, PM10 and PM2.5 for 2019 and 2030. It is to be noted that the model results represent annual averaged urban background concentrations, not local hotspot concentrations.

For NO_2, 0.1% of the population is exposed to levels above the air quality objective in 2019, but in 2030 none of the population is exposed to exceedances. In relation to the WHO guideline 9% of the population is exposed to NO_2 levels above 10 µg/m^3 in 2019. This number decreased to 0.4% in 2030. A slight majority of the exposure contribution is from regional background. In the 2030 scenarios the urban contribution decreased more than the regional contribution, compared to 2019.

For PM10 1.4% of the population is exposed to levels above the environmental objective (and the WHO guideline as they are the same) in 2019. In 2030 the percentage is increased to 2.3% due to slightly higher regional background concentrations in the Malmö region. It is clear that the regional contribution is dominant, and in regards to urban contributions, the non-exhaust traffic emissions is the most important source.

Regarding PM2.5 there is no exposure to levels above the environmental objective of 10 µg/m^3, however 47% of the population is exposed to levels above 5 µg/m^3 in 2019 and 35% in 2030. The regional contribution is very dominant, and in regards to urban contributions, several sources contribute significantly. Small-scale residential heating is the largest sector contributor to the urban exposure, followed by other urban sources.

5.3 Health impacts

The 2019 exposure was used to calculate preterm mortality assuming effects down to the lowest concentrations. A higher relative risk for PM2.5 was assumed for urban sources than for the regional background. An impact on mortality was assumed only from the urban contribution of NO_2 above the regional background. When adding preterm deaths per year attributed to regional and urban PM2.5 exposure, the total number becomes 4 264 deaths. When the yearly number of preterm deaths attributed to urban sources of both PM2.5 and NO_2 were added, the total number of deaths becomes 1 396.

These estimates for 2019 are lower than in a parallel study where the modelled exposure levels were higher (Gustavsson et al, 2022). At the same time these estimates are considerably higher than numbers reported for Sweden in reports from the European Environmental Agency, for example in ETC-HE Report 2022/10 (Soares J et al, 2022). In that report the main results are based on the estimated impacts on all-cause mortality in people over 30 years for concentrations above an annual PM2.5 of 5 µg/m^3 (using a 1×1 km^2 grid resolution), assuming a linear increase in the risk of mortality of 8% per 10 µg/m3, which for Sweden 2020 resulted in estimated 369 premature deaths due to exposure above 5 µg/m^3. When we for 2019 assumed an effect of PM2.5 on total mortality only above 5 µg/m^3 and the relative risk 1.08 per 10 µg/m^3, the estimated number became 417. However, we estimate as many as 3 542 preterm deaths per year with the same threshold combined with the relative risk reported for exposure levels <12 µg/m^3 in the large European ELAPSE Study (Strak et al, 2021).

It is striking how the estimated excess mortality is depending on the selected exposure-response function, and if it applied for all concentrations or only above a specific threshold. When the impacts in Sweden are assessed it is important to consider (1) how the relative risk increase with the concentration even at the lowest observed concentrations (Strak et al, 2021), (2) how the exposure-response relationship is steepest (highest effect estimates per concentration) at low concentrations (Vodonos et al 2018; Chen and Hoek, 2020; Strak et al, 2021), and (3), how the effect estimates become higher with more accurate exposure data (Vodonos et al, 2018; Segersson et al, 2021). Epidemiological results from research cohorts in Nordic countries suggests that it would be a serious mistake to follow the default assumptions chosen by EEA when countries like Sweden are studied.

The large influence of the selection of risk functions on the obtained results is of course also obvious when impacts on morbidity are estimated. For several of the outcomes included in this study there are alternative meta-coefficients available, and for stroke the applied relative risk seems to be higher than the potential alternatives.

6 References

Andersson, C., Langner, J., Bergström, R., 2007. Interannual variation and trends in air pollution over Europe due to climate variability during 1958–2001 simulated with a regional CTM coupled to the ERA40 reanalysis. Tellus B Chem. Phys. Meteorol. 59, 77–98. https://doi.org/10.1111/j.1600-0889.2006.00231.x

Andersson, C., Bergström, R., Bennet, C., Robertson, L., Thomas, M., Korhonen, H., Lehtinen, K.E.J., Kokkola, H., 2014. MATCH–SALSA – Multi-scale Atmospheric Transport and CHemistry model coupled to the SALSA aerosol microphysics model – Part 1: Model description and evaluation (preprint). Atmospheric Sciences. https://doi.org/10.5194/gmdd-7-3265-2014

Berkowicz et al., 2011: NO2 chemistry scheme in OSPM and other Danish models, Technical note, NERI, Aarhus university. http://www2.dmu.dk/AtmosphericEnvironment/Docs/NO2scheme.pdf

Brunekreef B, Strak M, Chen J, 2021. Mortality and Morbidity Effects of Long-term Exposure to Low-level PM2.5, BC, NO2, and O3: an analysis of European cohorts in the ELAPSE project. Res Rep Health Eff Inst. 208:1-127.

Chen J, Hoek G, 2020. Long-term exposure to PM and all-cause and cause-specific mortality: A systematic review and meta-analysis. Environ Int. 143:105974.

EEA (2022). Air quality in Europe 2022. Report no. 05/2022.

European Commission, Joint Research Centre, Janssen, S., Thunis, P., FAIRMODE guidance document on modelling quality objectives and benchmarking: version 3.3, Publications Office of the European Union, 2022. https://data.europa.eu/doi/10.2760/41988

ExternE (2005). Externalties of Energy – Methodology 2005 Update. Edited by Peter Bickel and Rainer Friedrich, European Commission EUR 21951.

Forsberg B, Lövenheim B, Sommar N J, Kriit H, Strömgren M, Johansson C (2021). Bättre metoder att beskriva hälsovinster av minskad luftföroreningsexponering från vägtrafik. Trafikverket (in Swedish).

GBD 2019 Risk Factors Collaborators, 2020. Global burden of 87 risk factors in 204 countries and territories, 1990-2019: a systematic analysis for the Global Burden of Disease Study 2019. Lancet 396(10258):1223-1249.

Gustafsson M, Lindén J, Tang L, Forsberg B, Orru H, Sjöberg K, Åström S (2018). Quantification of population exposure to NO2, PM2.5 and PM10 and estimated health impacts. IVL report C317.

Gustafsson M, Lindén J, Forsberg B, Åström S, Johansson E (2021). Quantification of population exposure to NO2, PM2.5 and PM10 and estimated health impacts 2019. IVL report B2446.

Héroux ME, Anderson HR, Atkinson R, Brunekreef B, Cohen A, Forastiere F, Hurley F, Katsouyanni K, Krewski D, Krzyzanowski M, Künzli N, Mills I, Querol X, Ostro B, Walton H, 2015. Quantifying the health impacts of ambient air pollutants: recommendations of a WHO/Europe project. Int J Public Health 60(5):619-27

Hoffmann B, Brunekreef B, Andersen ZJ, Forastiere F, Boogaard H, 2022. Benefits of future clean air policies in Europe: Proposed analyses of the mortality impacts of PM2.5 and NO2. Environ Epidemiol. 6(5):e221.

Hoek G, Krishnan RM, Beelen R, Peters A, Ostro B, Brunekreef B, Kaufman JD. (2013). Long-term air pollution exposure and cardio-respiratory mortality: a review. Environmental Health 2013;12:43.

Hult C, Merelli L, Mawdsley I, 2022. Styrmedel för minskade NOX-utsläpp från vägtrafik i scenarier med skärpta EU-krav för fordons CO2-utsläpp. IVL Report nr C 668.

Hvidtfeldt UA, Sørensen M, Geels C, Ketzel M, Khan J, Tjønneland A, Overvad K, Brandt J, Raaschou-Nielsen O, 2019. Long-term residential exposure to PM2.5, PM10, black carbon, NO2, and ozone and mortality in a Danish cohort. Environ Int. 123:265-272.

Huangfu P, Atkinson R, 2020. Long-term exposure to NO2 and O3 and all-cause and respiratory mortality: A systematic review and meta-analysis. Environ Int 144:105998.

Jerrett M, Burnett RT, Ma R, Pope CA 3rd, Krewski D, Newbold KB, Thurston G, Shi Y, Finkelstein N, Calle EE, Thun MJ, 2005. Spatial analysis of air pollution and mortality in Los Angeles. Epidemiology 16(6): 727-36.

Lefler JS, Higbee JD, Burnett RT, Ezzati M, Coleman NC, Mann DD, Marshall JD, Bechle M, Wang Y, Robinson AL, Arden Pope C 3rd, 2019. Air pollution and mortality in a large, representative U.S. cohort: multiple-pollutant analyses, and spatial and temporal decompositions. Environ Health 18(1):101.

Meister K, Johansson C, Forsberg B, 2012. Estimated short-term effects of coarse particles on daily mortality in Stockholm, Sweden. Environ Health Perspect. 120(3):431-6.

Nilsson Sommar J, Andersson EM, Andersson N, Sallsten G, Stockfelt L, Ljungman PL, Segersson D, Eneroth K, Gidhagen L, Molnar P, Wennberg P, Rosengren A, Rizzuto D, Leander K, Lager A, Magnusson PK, Johansson C, Barregard L, Bellander T, Pershagen G, Forsberg B, 2021. Long-term exposure to particulate air pollution and black carbon in relation to natural and cause-specific mortality: a multicohort study in Sweden. BMJ Open 11(9):e046040.

Omstedt, G., 2007: VEDAIR – ett internetverktyg för bedömning av luftkvalitet vid småskalig biobränsleeldning, SMHI Rapport nr. 123. http://urn.kb.se/resolve?urn=urn:nbn:se:smhi:diva-2215

Orellano P, Reynoso J, Quaranta N, Bardach A, Ciapponi A, 2020. Short-term exposure to particulate matter (PM10 and PM2.5), nitrogen dioxide (NO2), and ozone (O3) and all-cause and cause-specific mortality: Systematic review and meta-analysis. Environ Int. 142:105876.

Pinault L, Tjepkema M, Crouse DL, Weichenthal S, van Donkelaar A, Martin RV, Brauer M, Chen H, Burnett RT, 2016. Risk estimates of mortality attributed to low concentrations of ambient fine particulate matter in the Canadian community health survey cohort. Environ Health. 15:18.

Raaschou-Nielsen O, Andersen ZJ, Jensen SS, Ketzel M, Sørensen M, Hansen J, Loft S, Tjønneland A, Overvad K, 2012. Traffic air pollution and mortality from cardiovascular disease and all causes: a Danish cohort study. Env. Health 11:60.

Robertson, L., Langner, J., Engardt, M., 1999. An Eulerian Limited-Area Atmospheric Transport Model. J. Appl. Meteorol. 38, 190–210. https://journals.ametsoc.org/view/journals/apme/38/2/1520-0450_1999_038_0190_aelaat_2.0.co_2.xml

Segersson D, Eneroth K, Gidhagen L, Johansson C, Omstedt G, Nylén AE, Forsberg B, 2017. Health Impact of PM10, PM2.5 and Black Carbon Exposure Due to Different

Source Sectors in Stockholm, Gothenburg and Umea, Sweden. Int J Environ Res Public Health 14(7):742.

Segersson D, Johansson C, Forsberg B, 2021. Near-Source Risk Functions for Particulate Matter Are Critical When Assessing the Health Benefits of Local Abatement Strategies. Int J Environ Res Public Health 18(13):6847.

Segersson, D., 2021. Quantification of population exposure and health impacts associated with air pollution (PhD dissertation, Department of Environmental Science, Stockholm University). Retrieved from http://urn.kb.se/resolve?urn=urn:nbn:se:su:diva-199214

Segersson, D., Asker, C., Bennet, C., Andersson, C., 2021. Concentrations of NOx in Sweden over three decades using dispersion modelling at local and regional scale. Paper IV as part of dissertation. Retrieved from http://urn.kb.se/resolve?urn=urn:nbn:se:su:diva-199214

Soares J., González Ortiz A., Gsella A., Horálek J., Plass D., Kienzler S., 2022. Health Risk Assessment of Air Pollution and the Impact of the New WHO Guidelines. ETC-HE Report 2022/10, EEA.

Stieb D M, Berjawi R, Emode M, Zheng C, Salama D, Hocking R, Lyrette N, Matz C, Lavigne E, Shin H H, 2021. Systematic review and meta-analysis of cohort studies of long term outdoor nitrogen dioxide exposure and mortality. PLoS One 16(2):e0246451.

Strak M, Weinmayr G, Rodopoulou S, Chen J, de Hoogh K, Andersen ZJ, Atkinson R, Bauwelinck M, Bekkevold T, Bellander T, Boutron-Ruault MC, Brandt J, Cesaroni G, Concin H, Fecht D, Forastiere F, Gulliver J, Hertel O, Hoffmann B, Hvidtfeldt UA, Janssen NAH, Jöckel KH, Jørgensen JT, Ketzel M, Klompmaker JO, Lager A, Leander K, Liu S, Ljungman P, Magnusson PKE, Mehta AJ, Nagel G, Oftedal B, Pershagen G, Peters A, Raaschou-Nielsen O, Renzi M, Rizzuto D, van der Schouw YT, Schramm S, Severi G, Sigsgaard T, Sørensen M, Stafoggia M, Tjønneland A, Verschuren WMM, Vienneau D, Wolf K, Katsouyanni K, Brunekreef B, Hoek G, Samoli E, 2021. Long term exposure to low level air pollution and mortality in eight European cohorts within the ELAPSE project: pooled analysis. BMJ 374:n1904.

Söderqvist T, Kriit H K, Tidblad J, Andersson J, Jansson S-A, Svensson M, Wallström J, Andersson C, Orru H, Sommar N J, Forsberg B, 2019. Underlag för reviderade ASEK-värden för luftföroreningar: Slutrapport från projektet REVSEK (in Swedish). Trafikverket.

Thurston GD, Kipen H, Annesi-Maesano I, Balmes J, Brook RD, Cromar K, De Matteis S, Forastiere F, Forsberg B, Frampton MW, Grigg J, Heederik D, Kelly FJ, Kuenzli N, Laumbach R, Peters A, Rajagopalan ST, Rich D, Ritz B, Samet JM, Sandstrom T, Sigsgaard T, Sunyer J, Brunekreef B, 2017. A joint ERS/ATS policy statement: what constitutes an adverse health effect of air pollution? An analytical framework. Eur Respir J. 49(1):1600419.

Turner MC, Jerrett M, Pope CA 3rd, Krewski D, Gapstur SM, Diver WR, Beckerman BS, Marshall JD, Su J, Crouse DL, Burnett RT, 2016. Long-Term Ozone Exposure and Mortality in a Large Prospective Study. Am J Respir Crit Care Med. 193(10):1134-42.

WHO (2007). Health relevance of particulate matter from various sources. Report on a WHO Workshop Bonn, Germany, 26-27 March 2007.

WHO (2013a). Review of evidence on health aspects of air pollution – REVIHAAP Project Technical Report. Copenhagen, 2013.

WHO (2013b). Health risks of air pollution in Europe – HRAPIE. Recommendations for concentration-response functions for cost-benefit analysis of particulate matter, ozone and nitrogen dioxide. Copenhagen, 2013.

WHO (2016). Health risk assessment of air pollution. General principles.

WHO (2021). WHO global air quality guidelines. Particulate matter (PM 2.5 and PM10), ozone, nitrogen dioxide, sulfur dioxide and carbon monoxide. World Health Organization.

Vodonos A, Awad YA, Schwartz J, 2018. The concentration-response between long-term PM2.5 exposure and mortality; A meta-regression approach. Environ Res. 166:677-689.

7 Figures and tables

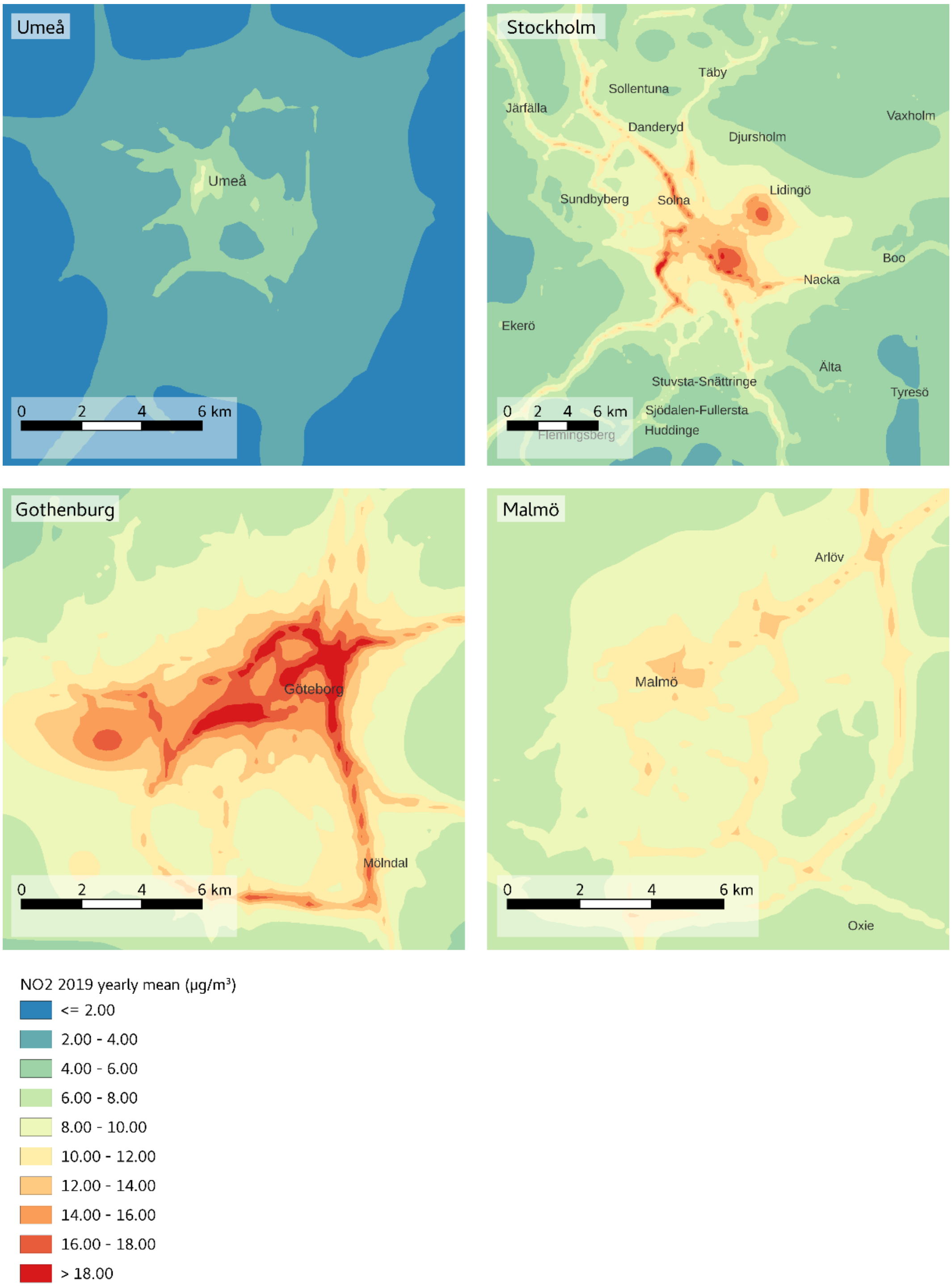

Figure 36. Annual mean concentrations of NO_2 in 2019 for the four cities of Malmö, Gothenburg, Stockholm and Umeå.

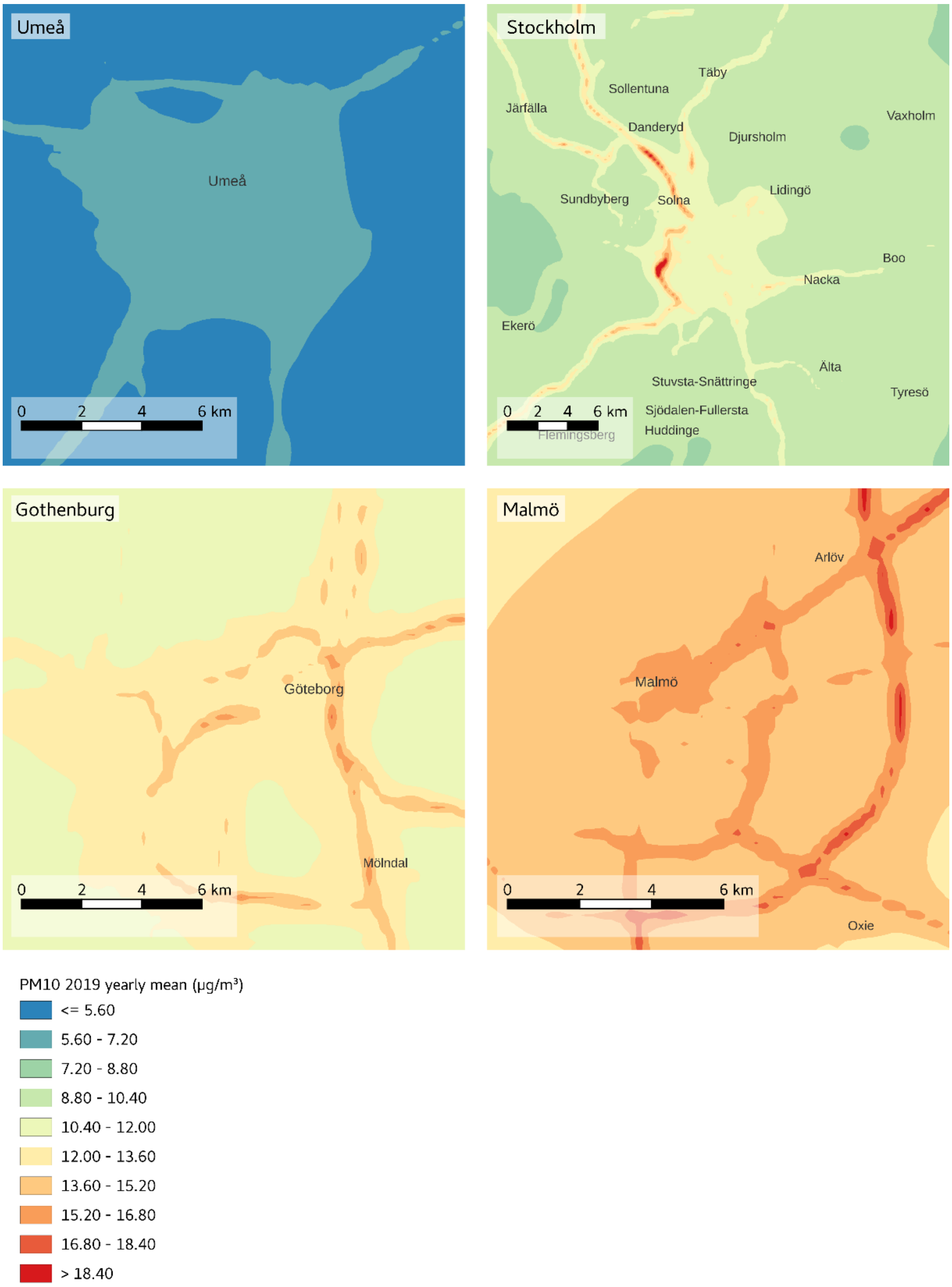

Figure 37. Annual mean concentrations of PM10 in 2019 for the four cities of Malmö, Gothenburg, Stockholm and Umeå.

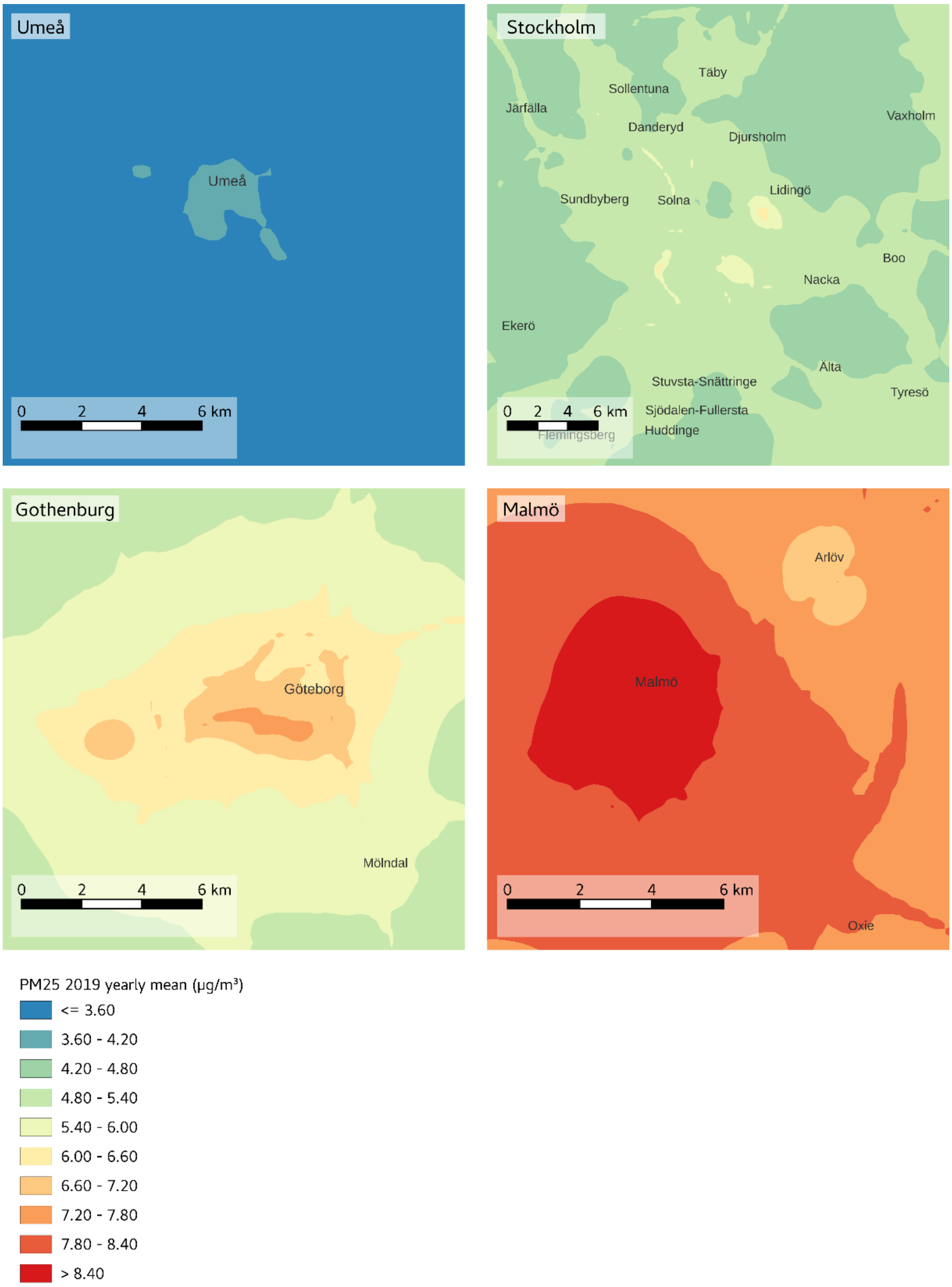

Figure 38. Annual mean concentrations of PM2.5 in 2019 for the four cities of Malmö, Gothenburg, Stockholm and Umeå.

8 SMHI Publications

SMHI publish seven report series. Three of these, the R-series, are intended for international readers and are in most cases written in English. For the others the Swedish language is used.

Name of the series	Published since
RMK (Report Meteorology and Climatology)	1974
RH (Report Hydrology)	1990
RO (Report Oceanography)	1986
METEOROLOGI	1985
HYDROLOGI	1985
OCEANOGRAFI	1985
KLIMATOLOGI	2009

Earlier issues published in serie RMK:

1 Thompson, T. Udin, I. and Omstedt, A. (1974)
Sea surface temperatures in waters surrounding Sweden

2 Bodin, S. (1974)
Development on an unsteady atmospheric boundary layer model

3 Moen, L. (1975)
A multi-level quasi-geostrophic model for short range weather predictions

4 Holmström, I. (1976)
Optimization of atmospheric models

5 Collins, W.G. (1976)
A parameterization model for calculation of vertical fluxes of momentum due to terrain induced gravity waves

6 Nyberg, A. (1976)
On transport of sulphur over the North Atlantic

7 Lundqvist, J-E. Udin, I. (1977)
Ice accretion on ships with special emphasis on Baltic conditions

8 Eriksson, B. (1977)
Den dagliga och årliga variationen av temperatur, fuktighet och vindhastighet vid några orter i Sverige

9 Holmström, I. and Stokes, J. (1978)
Statistical forecasting of sea level changes in the Baltic

10 Omstedt, A. and Sahlberg, J. (1978)
Some results from a joint Swedish-Finnish sea ice experiment, March, 1977

11 Haag, T. (1978)
Byggnadsindustrins väderberoende, seminarieuppsats i företagsekonomi, B-nivå

12 Eriksson, B. (1978)
Vegetationsperioden i Sverige beräknad från temperaturobservationer

13 Bodin, S. (1979)
En numerisk prognosmodell för det atmosfäriska gränsskiktet, grundad på den turbulenta energiekvationen

14 Eriksson, B. (1979)
Temperaturfluktuationer under senaste 100 åren

15 Udin, I. och Mattisson, I. (1979)
Havsis- och snöinformation ur datorbearbetade satellitdata - en modellstudie

16 Eriksson, B. (1979)
Statistisk analys av nederbördsdata. Del I. Arealnederbörd

17 Eriksson, B. (1980)
Statistisk analys av nederbördsdata. Del II. Frekvensanalys av månadsnederbörd

18 Eriksson, B. (1980)
Årsmedelvärden (1931-60) av nederbörd, avdunstning och avrinning

19 Omstedt, A. (1980)
A sensitivity analysis of steady, free floating ice

20 Persson, C. och Omstedt, G. (1980)
En modell för beräkning av luftföroreningars spridning och deposition på mesoskala.

21 Jansson, D. (1980)
Studier av temperaturinversioner och vertikal vindskjuvning vid Sundsvall-Härnösands flygplats

22 Sahlberg, J. and Törnevik, H. (1980)
A study of large scale cooling in the Bay of Bothnia

23 Ericson, K. and Hårsmar, P.-O. (1980)
Boundary layer measurements at Klockrike Oct 1977

24 Bringfelt, B. (1980)
A comparison of forest evapotranspiration determined by some independent methods

25 Bodin, S. and Fredriksson, U. (1980)
Uncertainty in wind forecasting for wind power networks

26 Eriksson, B. (1980)
Graddagsstatistik för Sverige

27 Eriksson, B.(1981)
Statistisk analys av nederbördsdata. Del III. 200-åriga nederbördsserier

28 Eriksson, B. (1981)
Den "potentiella" evapotranspirationen i Sverige

29 Pershagen, H. (1981)
Maximisnödjup i Sverige
(perioden 1905-70)

30 Lönnqvist, O. (1981)
Nederbördsstatistik med praktiska tillämpningar
(Precipitation statistics with practical applications.)

31 Melgarejo, J.W. (1981)
Similarity theory and resistance laws for the atmospheric boundary layer

32 Liljas, E. (1981)
Analys av moln och nederbörd genom automatisk klassning av AVHRR-data

33 Ericson, K. (1982)
Atmospheric boundary layer field experiment in Sweden 1980, GOTEX II,
part I

34 Schoeffler, P. (1982)
Dissipation, dispersion and stability of numerical schemes for advection and diffusion

35 Undén, P. (1982)
The Swedish Limited Area Model. Part A. Formulation

36 Bringfelt, B. (1982)
A forest evapotranspiration model using synoptic data

37 Omstedt, G. (1982)
Spridning av luftförorening från skorsten i konvektiva gränsskikt

38 Törnevik, H. (1982)
An aerobiological model for operational forecasts of pollen concentration in the air

39 Eriksson, B. (1982)
Data rörande Sveriges temperaturklimat.

40 Omstedt, G. (1984)
An operational air pollution model using routine meteorological data

41 Persson, C. and Funkquist, L. (1984)
Local scale plume model for nitrogen oxides. Model description

42 Gollvik, S. (1984)
Estimation of orographic precipitation by dynamical interpretation of synoptic model data

43 Lönnqvist, O. (1984)
Congression - A fast regression technique with a great number of functions of all predictors

44 Laurin, S. (1984)
Population exposure to SO and NO_x from different sources in Stockholm

45 Svensson, J. (1985)
Remote sensing of atmospheric temperature profiles by TIROS Operational Vertical Sounder

46 Eriksson, B. (1986)
Nederbörds- och humiditetsklimat i Sverige under vegetationsperioden

47 Taesler, R. (1986)
Köldperioden av olika längd och förekomst

48 Wu Zengmao (1986)
Numerical study of lake-land breeze over Lake Vättern, Sweden

49 Wu Zengmao (1986)
Numerical analysis of initialization procedure in a two-dimensional lake breeze model

50 Persson, C. (1986)
Local scale plume model for nitrogen oxides. Verification

51 Melgarejo, J.W. (1986)
An analytical model of the boundary layer above sloping terrain with an application to observations in Antarctica

52 Bringfelt, B. (1986)
Test of a forest evapotranspiration model

53 Josefsson, W. (1986)
Solar ultraviolet radiation in Sweden

54 Dahlström, B. (1986)
Determination of areal precipitation for the Baltic Sea

55 Persson, C. Rodhe, H. and De Geer, L-E. (1986)
The Chernobyl accident - A meteorological analysis of how radionucleides reached Sweden

56 Persson, C. Robertson, L. Grennfelt, P. Kindbom, K. Lövblad, G. Svanberg, P.-A. (1987)
Luftföroreningsepisoden över södra Sverige 2 - 4 februari 1987

57 Omstedt, G. (1988)
An operational air pollution model

58 Alexandersson, H. and Eriksson, B. (1989)
Climate fluctuations in Sweden 1860 - 1987

59 Eriksson, B. (1989)
Snödjupsförhållanden i Sverige - Säsongerna 1950/51 - 1979/80

60 Omstedt, G. and Szegö, J. (1990)
Människors exponering för luftföroreningar

61 Mueller, L. Robertson, L. Andersson, E. and Gustafsson, N. (1990)
Mesoscale objective analysis of near surface temperature, humidity and wind. And its application in air pollution modelling

62 Andersson, T. and Mattisson, I. (1991)
A field test of thermometer screens

63 Alexandersson, H. Gollvik, S. and Meuller, L. (1991)
An energy balance model for prediction of surface temperatures

64 Alexandersson, H. and Dahlström, B. (1992)
Future climate in the Nordic region - survey and synthesis for the next century

65 Persson, C. Langner, J. and Robertson, L. (1994)
Regional spridningsmodell för Göteborgs och Bohus, Hallands och Älvsborgs län.
A mesoscale air pollution dispersion model for the Swedish west-coast region
(In Swedish with captions also in English)

66 Karlsson, K.-G. (1994)
Satellite-estimated cloudiness from NOAA AVHRR data in the Nordic area during 1993

67 Karlsson, K-G. (1996)
Cloud classifications with the SCANDIA model

68 Persson, C. and Ullerstig, A. (1996)
Model calculations of dispersion of lindane over Europe. Pilot study with comparisons to measurements around the Baltic Sea and the Kattegatt

69 Langner, J. Persson, C. Robertson, L. and Ullerstig, A. (1996)
Air pollution Assessment Study Using the MATCH Modelling System. Application to sulphur and nitrogen compounds over Sweden 1994

70 Robertson, L. Langner, J. and Engardt, M. (1996)
MATCH - Meso-scale Atmospheric Transport and Chemistry modelling system

71 Josefsson, W. (1996)
Five years of solar UV-radiation monitoring in Sweden

72 Persson, C. Ullerstig, A. Robertson, L. Kindbom, K. and Sjöberg, K. (1996)
The Swedish Precipitation Chemistry Network. Studies in network design using the MATCH modelling system and statistical methods

73 Robertson, L. (1996)
Modelling of anthropogenic sulphur deposition to the African and South American continents

74 Josefsson, W. (1996)
Solar UV-radiation monitoring 1996

75 Häggmark, L. Ivarsson, K.-I. Olofsson, P.-O. (1997)
MESAN - Mesoskalig analys

76 Bringfelt, B. Backström, H. Kindell, S. Omstedt, G. Persson, C. and Ullerstig, A. (1997)
Calculations of PM-10 concentrations in Swedish cities- Modelling of inhalable particles

77 Gollvik, S. (1997)
The Teleflood project, estimation of precipitation over drainage basins

78 Persson, C. and Ullerstig, A. (1997)
Regional luftmiljöanalys för Västmanlands län baserad på MATCH modell-beräkningar och mätdata - Analys av 1994 års data

79 Josefsson, W. and Karlsson, J.-E. (1997)
Measurements of total ozone 1994-1996

80 Rummukainen, M. (1997)
Methods for statistical downscaling of GCM simulations

81 Persson, T. (1997)
Solar irradiance modelling using satellite retrieved cloudiness - A pilot study

82 Langner, J. Bergström, R. and Pleijel, K. (1998)
European scale modelling of sulfur, oxidized nitrogen and photochemical oxidants. Model

development and evaluation for the 1994 growing season

83 Rummukainen, M. Räisänen, J. Ullerstig, A. Bringfelt, B. Hansson, U. Graham, P. and Willén, U. (1998)
RCA - Rossby Centre regional Atmospheric climate model: model description and results from the first multi-year simulation

84 Räisänen, J. and Doescher, R. (1998)
Simulation of present-day climate in Northern Europe in the HadCM2 OAGCM

85 Räisänen, J. Rummukainen, M. Ullerstig, A. Bringfelt, B. Hansson, U. and Willén. U. (1999)
The First Rossby Centre Regional Climate Scenario - Dynamical Downscaling of CO_2-induced Climate Change in the HadCM2 GCM

86 Rummukainen, M. (1999)
On the Climate Change debate

87 Räisänen, J. (2000)
CO_2-induced climate change in northern Europe: comparison of 12 CMIP2 experiments

88 Engardt, M. (2000)
Sulphur simulations for East Asia using the MATCH model with meteorological data from ECMWF

89 Persson, T. (2000)
Measurements of Solar Radiation in Sweden 1983-1998

90 Michelson, D. B. Andersson, T. Koistinen, J. Collier, C. G. Riedl, J. Szturc, J. Gjertsen, U. Nielsen, A. and Overgaard, S. (2000)
BALTEX Radar Data Centre Products and their Methodologies

91 Josefsson, W. (2000)
Measurements of total ozone 1997 – 1999

92 Andersson, T. (2000)
Boundary clear air echoes in southern Sweden

93 Andersson, T. (2000)
Using the Sun to check some weather radar parameters

94 Rummukainen, M. Bergström, S. Källén, E. Moen, L. Rodhe, J. and Tjernström, M. (2000)
SWECLIM – The First Three Years

95 Meier, H. E. M. (2001)
The first Rossby Centre regional climate scenario for the Baltic Sea using a 3D coupled ice-ocean model

96 Landelius, T. Josefsson, W. and Persson, T. (2001)
A system for modelling solar radiation parameters with mesoscale spatial resolution

97 Karlsson, K.-G. (2001)
A NOAA AVHRR cloud climatology over Scandinavia covering the period 1991-2000

98 Bringfelt, B. Räisänen, J. Gollvik, S. Lindström, G. Graham, P. and Ullerstig, A. (2001)
The land surface treatment for the Rossby Centre Regional Atmospheric Climate Model - version 2 (RCA2)

99 Kauker, F. and Meier, H E M. (2002)
Reconstructing atmospheric surface data for the period 1902-1998 to force a coupled ocean-sea ice model of the Baltic Sea

100 Klein, T. Bergström, R. and Persson, C. (2002)
Parameterization of dry deposition in MATCH

101 Räisänen, J. Hansson, U. Ullerstig A. Doescher, R. Graham, L. P. Jones, C. Meier, M. Samuelsson, P. and Willén, U. (2003)
GCM driven simulations of recent and future climate with the Rossby Centre coupled atmosphere - Baltic Sea regional climate model RCAO

102 Tjernström, M. Rummukainen, M. Bergström, S. Rodhe, J. and Persson, G. (2003)
Klimatmodellering och klimatscenarier ur SWECLIMs perspektiv

103 Segersson, D. (2003)
Numerical Quantification of Driving Rain on Buildings

104 Rummukainen, M. and the SWECLIM participants (2003)
The Swedish regional climate modelling program 1996-2003 Final report

105 Robertson, L. (2004)
Extended back-trajectories by means of adjoint equations

106 Rummukainen, M. Bergström S. Persson G. Ressner, E. (2005)
Anpassningar till klimatförändringar

107 Will not be published

108 Kjellström, E. Bärring, L. Gollvik, S. Hansson, U. Jones, C. Samuelsson, P. Rummukainen, M. Ullerstig, A. Willén, U. Wyser, K. (2005)
A 140-year simulation of European climate with the new version of the Rossby Centre regional atmospheric climate model (RCA3)

109 Meier, H.E.M. Andréasson, J. Broman, B. Graham, L. P. Kjellström, E. Persson, G. and Viehhauser, M. (2006)
Climate change scenario simulations of wind, sea level, and river discharge in the Baltic Sea

and Lake Mälaren region – a dynamical downscaling approach from global to local scales

110 Wyser, K. Rummukainen, M. Strandberg, G. (2006)
Nordic regionalisation of a greenhouse-gas stabilisation scenario

111 Persson, G. Bärring, L. Kjellström, E. Strandberg G. Rummukainen, M. (2007).
Climate indices for vulnerability assessments

112 Jansson, A. Persson, Ch. Strandberg, G. (2007)2D meso-scale re-analysis of precipitation, perature and wind over Europe -ERAMESAN

113 Lind, P. Kjellström, E. (2008)
Temperature and Precipitation changes in Sweden; a wide range of model-based projections for the 21st century

114 Klein, T. Karlsson, P-E. Andersson, S. Engardt, M. Sjöberg, K. (2011)
Assessing and improving the Swedish forecast and information capabilities for ground-level ozone

115 Andersson, C. Bergström, R. Bennet, C. Thomas, M. Robertson, L. SMHI. Kokkola, H. Korhonen, H. Lehtinen, K. FMI (2013)
MATCH-SALSA Multi-scale Atmospheric Transport and Chemistry model coupled to the SALSA aerosol microphysics model

116 Strandberg, G. Bärring, L. Hansson, U. Jansson, C. Jones, C. Kjellström, E. Kolax, M. Kupiainen, M. Nikulin, G. Samuelsson, P. Ullerstig, A. and Wang, S. (2014)
CORDEX scenarios for Europe from the Rossby Centre regional climate model RCA4

117 Lennart Bengtsson, Nils Gustafsson1), Bo Döös2), Daniel Söderman, Lars Moen3), Thomas Thompson4), Paul Jakobsson, Gunnar Bleckert, Ann-Beate Henriksson, Bo Lindgren5) and Per Kållberg
1)Correspondig author, e-mail: Nils.Gustafsson@smhi.se
2)Deceased 2010 3)Deceased 2006 4)Deceased 2015 5)Deceased 2005
The Meteorological Auto Code (MAC) and Numerical Weather Prediction (NWP) at SMHI

118 Sandra Andersson, Lars Bärring, Tomas Landelius, Patrick Samuelsson, Sejmon Schimanke (2021)
SMHI Gridded Climatology

Swedish Meteorological and Hydrological Institute
SE 601 76 NORRKÖPING
Phone +46 11-495 80 00 Telefax +46 11-495 80 01

ISSN: 0347-2116